J|A|C|S ARTICLES

Published on Web 03/18/2009

# Interlocked Host Anion Recognition by an Indolocarbazole-Containing [2]Rotaxane

Asha Brown,[†] Kathleen M. Mullen,[†] Jay Ryu,[†] Michał J. Chmielewski,[†] Sérgio M. Santos,[‡] Vitor Felix,[‡] Amber L. Thompson,[†] John E. Warren,[§,||] Sofia I. Pascu,[||] and Paul D. Beer*,[†]

*Chemistry Research Laboratory, Department of Chemistry, University of Oxford, Mansfield Road, Oxford, OX1 3TA U.K., Departamento de Química, CICECO and Secção Autónoma de Ciências da Saúde, Universidade de Aveiro, 3810-193 Aveiro, Portugal, Synchrotron Radiation Source, Daresbury Laboratory, Warrington, WA4 4AD U.K., and Department of Chemistry, University of Bath, Bath, BA2 7AY U.K.*

Received December 19, 2008; E-mail: paul.beer@chem.ox.ac.uk

***Abstract:*** The design, synthesis, structure, and anion-binding properties of the first indolocarbazole-containing interlocked structure are described. The novel [2]rotaxane molecular structure incorporates a neutral indolocarbazole-containing axle component which is encircled by a tetracationic macrocycle functionalized with an isophthalamide anion recognition motif. $^1$H NMR and UV−visible spectroscopies and X-ray crystallography demonstrated the importance of $\pi$-donor−acceptor, CH$\cdots\pi$, and electrostatic interactions in the assembly of pseudorotaxanes between the electron-deficient tetracationic macrocycle and a series of $\pi$-electron-rich indolocarbazole derivatives. Subsequent urethane stoppering of one of these complexes afforded a [2]rotaxane, which was shown by $^1$H NMR spectroscopic titration experiments to exhibit enhanced chloride and bromide anion recognition compared to its non-interlocked components. Computational molecular dynamics simulations provide further insight into the mechanism and structural nature of the anion recognition process, confirming it to involve cooperative hydrogen-bond donation from both macrocycle and indolocarbazole components of the rotaxane. The observed selectivity of the [2]rotaxane for chloride is interpreted in terms of its unique interlocked binding cavity, defined by the macrocycle isophthalamide and indolocarbazole N−H protons, which is complementary in size and shape to this halide guest.

## Introduction

Stimulated by the fundamental roles played by negatively charged species in a range of biological, chemical, medical, and environmental processes, the interest being shown in the syntheses of receptor systems designed to recognize and sense anions has increased rapidly in recent years.[1] In particular, various hydrogen-bond donor groups such as amide,[2−4] urea,[5] thiourea,[6] hydroxyl,[7] and pyrrole[8] incorporated into acyclic and macrocyclic structural frameworks have been exploited extensively in this regard.

In spite of the precedent of Nature using the tryptophan group as an efficient hydrogen-bond donor to recognize sulfate in the

[†] University of Oxford.
[‡] Universidade de Aveiro.
[§] Daresbury Laboratory.
[||] University of Bath.

(1) Bianchi, A.; Bowman-James, K.; García-España, E. *Supramolecular Chemistry of Anions*; Wiley-VCH: New York, 1997. Sessler, J. L.; Gale, P. A.; Cho, W.-S. *Anion Receptor Chemistry*; RSC: Cambridge, 2006. Schmidtchen, F. P.; Berger, M. *Chem. Rev.* **1997**, *97*, 1609–1646. Beer, P. D.; Gale, P. A. *Angew. Chem., Int. Ed.* **2001**, *40*, 486–516. Best, M. D.; Tobey, S. L.; Anslyn, E. V. *Coord. Chem. Rev.* **2003**, *240*, 3–15. Llinares, J. M.; Powell, D.; Bowman-James, K. *Coord. Chem. Rev.* **2003**, *240*, 57–75. Choi, K.; Hamilton, A. D. *Coord. Chem. Rev.* **2003**, *240*, 101–110. Wedge, T. J.; Hawthorne, M. F. *Coord. Chem. Rev.* **2003**, *240*, 111–128. Davis, A. P.; Joos, J.-B. *Coord. Chem. Rev.* **2003**, *240*, 143–156. Beer, P. D.; Hayes, E. J. *Coord. Chem. Rev.* **2003**, *240*, 167–189. Martinez-Manez, R.; Sancenon, F. *Chem. Rev.* **2003**, *103*, 4419–4476. Filby, M. H.; Steed, J. W. *Coord. Chem. Rev.* **2006**, *250*, 3200–3218. Davis, A. P. *Coord. Chem. Rev.* **2006**, *250*, 2939–2951. García-España, E.; Díaz, P.; Llinares, J. M.; Bianchi, A. *Coord. Chem. Rev.* **2006**, *250*, 2952–2986. Wichmann, K.; Antonioli, B.; Söhnel, T.; Wenzel, M.; Gloe, K.; Gloe, K.; Price, J. R.; Lindoy, L. F.; Blake, A. J.; Schröder, M. *Coord. Chem. Rev.* **2006**, *250*, 2987–3003. Katayev, E. A.; Ustynyuk, Y. A.; Sessler, J. L. *Coord. Chem. Rev.* **2006**, *250*, 3004–3037. O'Neil, E. J.; Smith, B. D. *Coord. Chem. Rev.* **2006**, *250*, 3068–3080. Martínez-Máñez, R.; Sancenón, F. *Coord. Chem. Rev.* **2006**, *250*, 3081–3093. Gunnlaugsson, T.; Glynn, M.; Tocci, G. M.; Kruger, P. E.; Pfeffer, F. M. *Coord. Chem. Rev.* **2006**, *250*, 3094–3117. Rice, C. R. *Coord. Chem. Rev.* **2006**, *250*, 3190–3199. Gale, P. A.; Quesada, R. *Coord. Chem. Rev.* **2006**, *250*, 3219–3244. Gale, P. A.; Garcia-Garrido, S. E.; Garric, J. *Chem. Soc. Rev.* **2008**, *37*, 151–190.

(2) Kavallieratos, K.; de Gala, S. R.; Austin, D. J.; Crabtree, R. H. *J. Am. Chem. Soc.* **1997**, *119*, 2325–2326. Kavallieratos, K.; Bertao, C. M.; Crabtree, R. H. *J. Org. Chem.* **1999**, *64*, 1675–1683.

(3) Chmielewski, M. J.; Jurczak, J. *Chem. Eur. J.* **2005**, *11*, 6080–6094. Chmielewski, M. J.; Jurczak, J. *Chem. Eur. J.* **2006**, *12*, 7652–7667.

(4) Bondy, C. R.; Loeb, S. J. *Coord. Chem. Rev.* **2003**, *240*, 77–99. Kang, S. O.; Begum, R. A.; Bowman-James, K. *Angew. Chem., Int. Ed.* **2006**, *45*, 7882–7894.

(5) Esteban-Gomez, D.; Fabbrizzi, L.; Licchelli, M. *J. Org. Chem.* **2005**, *70*, 5717–5720. Fan, E.; Van Arman, S. A.; Kincaid, S.; Hamilton, A. D. *J. Am. Chem. Soc.* **1993**, *115*, 369–370.

(6) Lee, K. H.; Hong, J.-I. *Tetrahedron Lett.* **2000**, *41*, 6083–6087. Garcia-Garrido, S. E.; Caltagirone, C.; Light, M. E.; Gale, P. A. *Chem. Commun.* **2007**, 1450–1452. Duke, R. M.; Gunnlaugsson, T.; O'Brien, J. E.; McCabe, T. *Org. Biomol. Chem.* **2008**, *6*, 4089–4092.

  

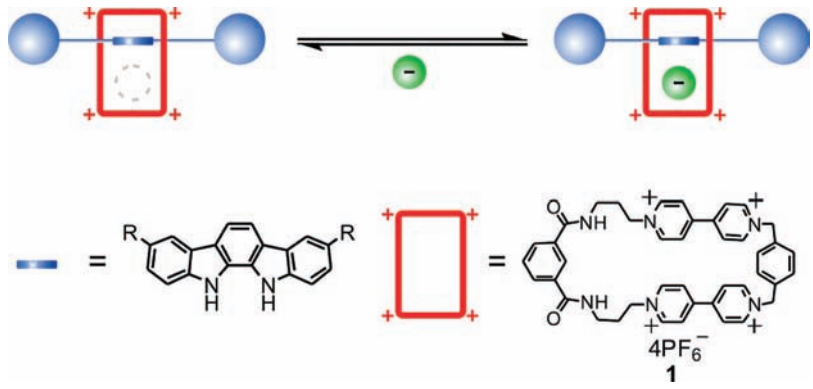


***Figure 1.*** Schematic representation of the target interlocked anion host system.

cavity of the sulfate-binding protein,[9] it is only during the last three years that the indole motif has begun to attract its deserved attention in anion receptor design research.[10] For example, seminal papers by the groups of Jeong,[11−13] Sessler,[14] and Gale[15] have demonstrated that indole- or biindole-containing receptors display strong binding affinities and high degrees of selectivity for anions.

With the aim of manipulating the unique topological cavities of mechanically bonded molecules in host−guest chemistry, an approach which is underexploited,[16] especially for anion recognition applications,[17] we have developed general methods of using anions to template the formation of interpenetrated and interlocked structures.[18] Indolo[2,3-*a*]carbazoles are a new family of anion receptors which bind anions strongly *via* their two preorganized hydrogen-bond-donating pyrrole groups.[11,12,19] They are attractive building blocks for the potential construction of interpenetrative assemblies because of their rodlike shape. Indeed, very recently we have reported the unprecedented anion templation of a neutral pseudorotaxane assembly using an indolocarbazole threading component.[20] In this paper we describe the first example of an indolocarbazole-containing interlocked molecular structure, a novel [2]rotaxane whose interlocked binding domain is shown to exhibit enhanced chloride and bromide anion-binding affinity compared to the individual axle and macrocycle components. In addition, computational molecular dynamics simulations are used to explain the observed anion selectivity trends and elucidate the cooperative structural nature of the orthogonal indolocarbazole axle and isophthalamide macrocycle rotaxane binding components in the anion recognition process.

## Results and Discussion

**Design and Synthetic Strategy.** The design of the target [2]rotaxane encompasses an indolocarbazole-containing axle and a macrocycle functionalized with an anion recognition motif. Interlocking the two components should generate a host system capable of recognizing anionic guest species in a cooperative manner with high binding affinity and selectivity within its unique interlocked binding cavity (Figure 1).

Indolocarbazole is a $\pi$-electron-rich aromatic system which requires a macrocycle possessing an electron-deficient cavity for interpenetrative assembly. In search of a suitable electron-deficient system, we turned to the 4,4′-bipyridinium moiety.

(7) Winstanley, K. J.; Sayer, A. M.; Smith, D. K. *Org. Biomol. Chem.* **2006**, *4*, 1760–1767. Wu, J. S.; Zhou, J. H.; Wang, P. F.; Zhang, X. H.; Wu, S. K. *Org. Lett.* **2005**, *7*, 2133–2136. Davis, A. P.; Perry, J. J.; Warham, R. S. *Tetrahedron Lett.* **1998**, *39*, 4569–4572. Davis, A. P.; Gilmer, J. F.; Perry, J. J. *Angew. Chem., Int. Ed. Engl.* **1996**, *35*, 1312–1315.
(8) Sessler, J. L.; An, D.; Cho, W. S.; Lynch, V.; Yoon, D. W.; Hong, S. J.; Lee, C. H. *J. Org. Chem.* **2005**, *70*, 1511–1517. Yin, Z. M.; Zhang, Y. H.; He, J. Q.; Cheng, J. P. *Tetrahedron* **2006**, *62*, 765–770. Sessler, J. L.; Camiolo, S.; Gale, P. A. *Coord. Chem. Rev.* **2003**, *240*, 17–55. Anzenbacher, J. P.; Nishiyabu, R.; Palacios, M. A. *Coord. Chem. Rev.* **2006**, *250*, 2929–2938. Sessler, J. L.; Davis, J. M. *Acc. Chem. Res.* **2001**, *34*, 989–997.
(9) He, J. J.; Quiocho, F. A. *Science* **1991**, *251*, 1479–1481.
(10) Chmielewski, M. J.; Charon, M.; Jurczak, J. *Org. Lett.* **2004**, *6*, 3501–3504. Gale, P. A. *Chem. Commun.* **2008**, 4525–4540.
(11) Chang, K. J.; Moon, D.; Lah, M. S.; Jeong, K. S. *Angew. Chem., Int. Ed.* **2005**, *44*, 7926–7929. Chang, K. J.; Moon, D.; Lah, M. S.; Jeong, K. S. *Chem. Commun.* **2007**, 3401–3403. Chae, M. K.; Lee, J. I.; Kim, N. K.; Jeong, K. S. *Tetrahedron Lett.* **2007**, *48*, 6624–6627. Kwon, T. H.; Jeong, K. S. *Tetrahedron Lett.* **2006**, *47*, 8539–8541.
(12) Ju, J.; Park, M.; Suk, J.-m.; Lah, M. S.; Jeong, K.-S. *Chem. Commun.* **2008**, 3546–3548. Chang, K. J.; Chae, M. K.; Lee, C.; Lee, J. Y.; Jeong, K. S. *Tetrahedron Lett.* **2006**, *47*, 6385–6388. Nam-Kyun, K.; Kyoung-Jin, C.; Dohyun, M.; Soo, L. M.; Kyu-Sung, J. *Chem. Commun.* **2007**, 3401–3403.
(13) Suk, J. M.; Chae, M. K.; Kim, N. K.; Kim, U. I.; Jeong, K. S. *Pure Appl. Chem.* **2008**, *80*, 599–608. Lee, J. Y.; Lee, M. H.; Jeong, K. S. *Supramol. Chem.* **2007**, *19*, 257–263. Kim, N. K.; Chang, K. J.; Moon, D.; Lah, M. S.; Jeong, K. S. *Chem. Commun.* **2007**, 3401–3403. Suk, J.-m.; Jeong, K.-S. *J. Am. Chem. Soc.* **2008**, *130*, 11868–11869. Naidu, V. R.; Kim, M. C.; Suk, J.-M.; Kim, H.-J.; Lee, M.; Sim, E.; Jeong, K.-S. *Org. Lett.* **2008**, *10*, 5373–5376.
(14) Sessler, J. L.; Cho, D. G.; Lynch, V. *J. Am. Chem. Soc.* **2006**, *128*, 16518–16519. Piątek, P.; Lynch, V. M.; Sessler, J. L. *J. Am. Chem. Soc.* **2004**, *126*, 16073–16076.
(15) Bates, G. W.; Gale, P. A.; Light, M. E. *Chem. Commun.* **2007**, 2121–2123. Bates, G. W.; Triyanti; Light, M. E.; Albrecht, M.; Gale, P. A. *J. Org. Chem.* **2007**, *72*, 8921–8927. Caltagirone, C.; Gale, P. A.; Hiscock, J. R.; Brooks, S. J.; Hursthouse, M. B.; Light, M. E. *Chem. Commun.* **2008**, 3007–3009. Claudia Caltagirone, Jennifer, R. H.; Michael, B. H.; Mark, E. L.; Philip, A. G. *Chem. Eur. J.* **2008**, *14*, 10236–10243.
(16) Kameta, N.; Nagawa, Y.; Karikomi, M.; Hiratani, K. *Chem. Commun.* **2006**, 3714–3716. Nagawa, Y.; Suga, J.; Hiratani, K.; Koyama, E.; Kanesato, M. *Chem. Commun.* **2005**, 749–751. Hiratani, K.; Kaneyama, M.; Nagawa, Y.; Koyama, E.; Kanesato, M. *J. Am. Chem. Soc.* **2004**, *126*, 13568–13569. Smukste, I.; House, B. E.; Smithrud, D. B. *J. Org. Chem.* **2003**, *68*, 2559–2571. Lam, R. T. S.; Belenguer, A.; Roberts, S. L.; Naumann, C.; Jarrosson, T.; Otto, S.; Sanders, J. K. M. *Science* **2005**, *308*, 667–669.
(17) Deetz, M. J.; Shukla, R.; Smith, B. D. *Tetrahedron* **2002**, *58*, 799–805. Andrievsky, A.; Ahuis, F.; Sessler, J. L.; Vogtle, F.; Gudat, D.; Moini, M. *J. Am. Chem. Soc.* **1998**, *120*, 9712–9713. Curiel, D.; Beer, P. D. *Chem. Commun.* **2005**, 1909–1911. Bayly, S. R.; Gray, T. M.; Chmielewski, M. J.; Davis, J. J.; Beer, P. D. *Chem. Commun.* **2007**, 2234–2236.
(18) Beer, P. D.; Sambrook, M. R.; Curiel, D. *Chem. Commun.* **2006**, 2105–2117. Lankshear, M. D.; Beer, P. D. *Acc. Chem. Res.* **2007**, *40*, 657–668.
(19) Curiel, D.; Cowley, A.; Beer, P. D. *Chem. Commun.* **2005**, 236–238.
(20) Chmielewski, M. J.; Zhao, L.; Brown, A.; Curiel, D.; Sambrook, M. R.; Thompson, A. L.; Santos, S. M.; Felix, V.; Davis, J. J.; Beer, P. D. *Chem. Commun.* **2008**, 3154–3156.

***Scheme 1.*** Synthesis of Indolocarbazole Derivatives[a]

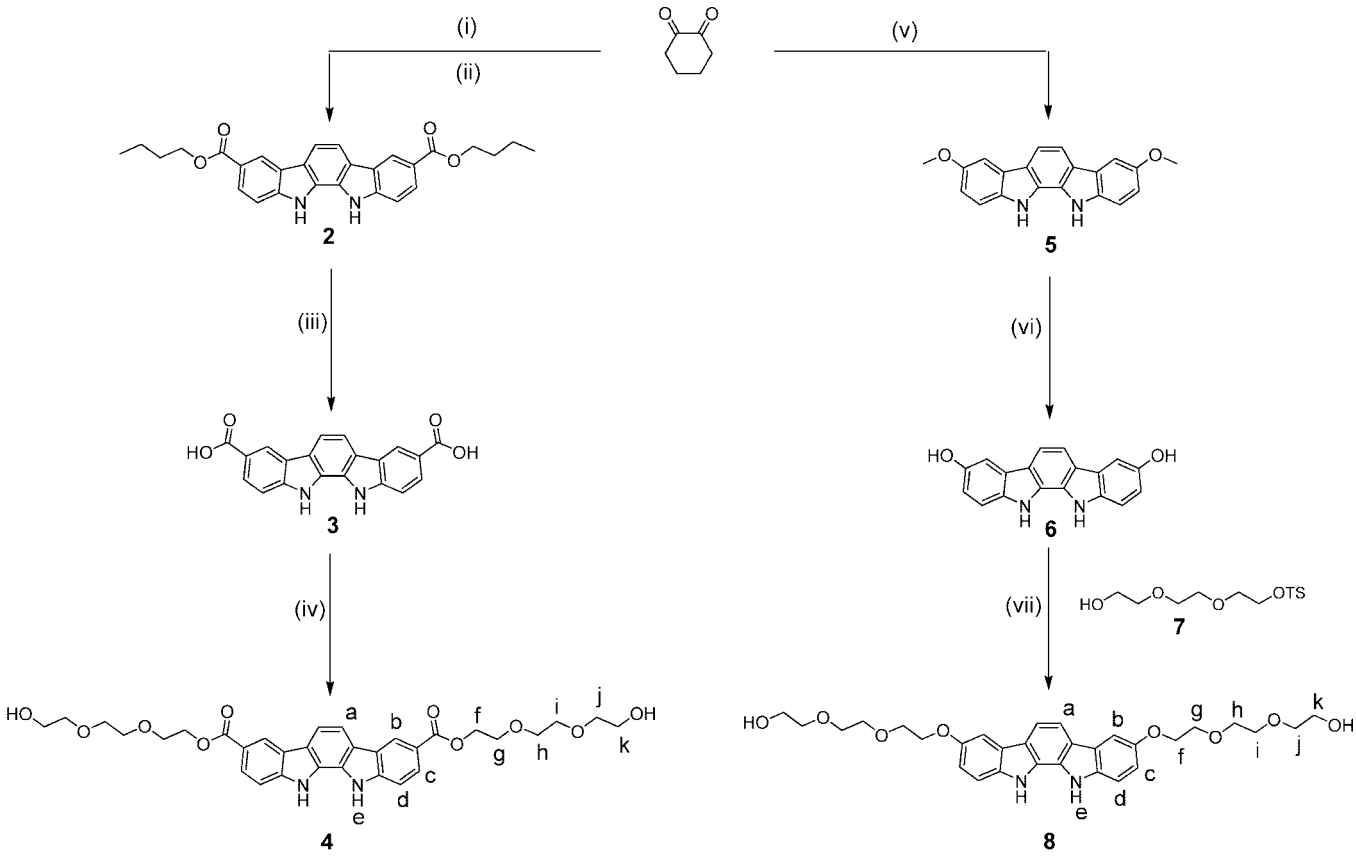


[a] Reagents and conditions: (i) 4-hydrazinebenzoic acid, $H_2SO_4$, nBuOH, reflux, 60 h; (ii) Pd/C, DMF, reflux, 24 h, 68%; (iii) KOH, iPrOH/$H_2O$, reflux, 24 h, 91%; (iv) 2-[2-(2-chloroethoxy)ethoxy]ethanol, $Et_3N$, DMF, 140 °C, microwave irradiation, 3 h, 69%; (v) 4-methoxyphenylhydrazine, $H_2SO_4$, EtOH, reflux, 24 h, 18%; (vi) $BBr_3$, $CH_2Cl_2$, −78 °C to room temperature, 18 h, 77%; (vii) $K_2CO_3$, DMF, 70 °C, 48 h, 16%.

Tetracationic macrocycles incorporating this system have been shown to include a range of $\pi$-electron-rich guests, including indole and its derivatives, by a combination of charge transfer and CH···$\pi$ interactions.[21,22] The isophthalamide motif,[2] which has previously been exploited in the anion-templated synthesis of interlocked structures containing topologically constrained binding cavities,[23,24] was chosen as the anion recognition fragment of the macrocycle. Hence, the requirement for incorporation of both positively charged bipyridinium and isophthalamide hydrogen-bond-donor functional groups into a cyclic structure led to the design of macrocycle **1**.

**Synthesis.** Indolocarbazole derivatives **4** and **8** (Scheme 1) were targeted as potential thread components, as their terminal hydroxyl groups provide suitable functionality for rotaxane synthesis *via* stoppering methodologies. The bis-ester **2** was prepared in 68% yield by a double Fischer indolization of 1,2-cyclohexanedione with 4-hydrazinebenzoic acid in *n*-butanol followed by dehydrogenation catalyzed by Pd/C in refluxing DMF. The bis-acid **3** was obtained in 91% yield by subsequent base-catalyzed hydrolysis of the ester (KOH, iPrOH/$H_2O$). A microwave-assisted reaction of compound **3** with 2-[2-(2-chloroethoxy)ethoxy]ethanol in DMF in the presence of $Et_3N$ afforded compound **4** in 69% yield. 3,8-Dimethoxyindolocarbazole **5** was prepared in 18% yield by reaction of 1,2-cyclohexanedione with 4-methoxyphenylhydrazine in acidified ethanol. Treatment with $BBr_3$ in $CH_2Cl_2$ afforded the bis-hydroxy indolocarbazole derivative **6** in 77% yield. This was alkylated with monotosylated ethylene glycol derivative **7** to give compound **8** in 16% yield.

The new tetracationic macrocycle **1** was synthesized in three steps according to Scheme 2. Dibromo derivative **9** was prepared in 35% yield by condensation of isophthaloyl dichloride with 3-bromopropylamine. Reaction of compound **9** with an excess of 4,4′-bipyridine in refluxing $CH_3CN$ gave the macrocycle precursor **10** in 73% yield after anion exchange. This was reacted with 1,4-bis(bromomethyl)benzene under high-dilution

(21) Mirzoian, A.; Kaifer, A. E. *J. Org. Chem.* **1995**, *60*, 8093–8095.
(22) Philp, D.; Slawin, A. M. Z.; Spencer, N.; Stoddart, J. F.; Williams, D. J. *J. Chem. Soc., Chem. Commun.* **1991**, 1584–1586. Asakawa, M.; Ashton, P. R.; Balzani, V.; Brown, C. L.; Credi, A.; Matthews, O. A.; Newton, S. P.; Raymo, F. M.; Shipway, A. N.; Spencer, N.; Quick, A.; Stoddart, J. F.; White, A. J. P.; Williams, D. J. *Chem. Eur. J.* **1999**, *5*, 860–875. Claessens, C. G.; Stoddart, J. F. *J. Phys. Org. Chem.* **1997**, *10*, 254–272. Asakawa, M.; Ashton, P. R.; Menzer, S.; Raymo, F. M.; Stoddart, J. F.; White, A. J. P.; Williams, D. J. *Chem. Eur. J.* **1996**, *2*, 877–893. Ballardini, R.; Balzani, V.; Dehaen, W.; Dell'Erba, A. E.; Raymo, F. M.; Stoddart, J. F.; Venturi, M. *Eur. J. Org. Chem.* **2000**, 591–602. Anelli, P. L.; et al. *Chem. Eur. J.* **1997**, *3*, 1113–1135. Asakawa, M.; Brown, C. L.; Pasini, D.; Stoddart, J. F.; Wyatt, P. G. *J. Org. Chem.* **1996**, *61*, 7234–7235. Goodnow, T. T.; Reddington, M. V.; Stoddart, J. F.; Kaifer, A. E. *J. Am. Chem. Soc.* **1991**, *113*, 4335–4337.
(23) Ng, K. Y.; Felix, V.; Santos, S. M.; Rees, N. H.; Beer, P. D. *Chem. Commun.* **2008**, 1281–1283. Lankshear, M. D.; Evans, N. H.; Bayly, S. R.; Beer, P. D. *Chem. Eur. J.* **2007**, *13*, 3861–3870. Sambrook, M. R.; Beer, P. D.; Lankshear, M. D.; Ludlow, R. F.; Wisner, J. A. *Org. Biomol. Chem.* **2006**, *4*, 1529–1538. Sambrook, M. R.; Beer, P. D.; Wisner, J. A.; Paul, R. L.; Cowley, A. R. *J. Am. Chem. Soc.* **2004**, *126*, 15364–15365.
(24) Wisner, J. A.; Beer, P. D.; Drew, M. G. B.; Sambrook, M. R. *J. Am. Chem. Soc.* **2002**, *124*, 12469–12476.

***Scheme 2.*** Synthesis of Macrocycle **1**[a]

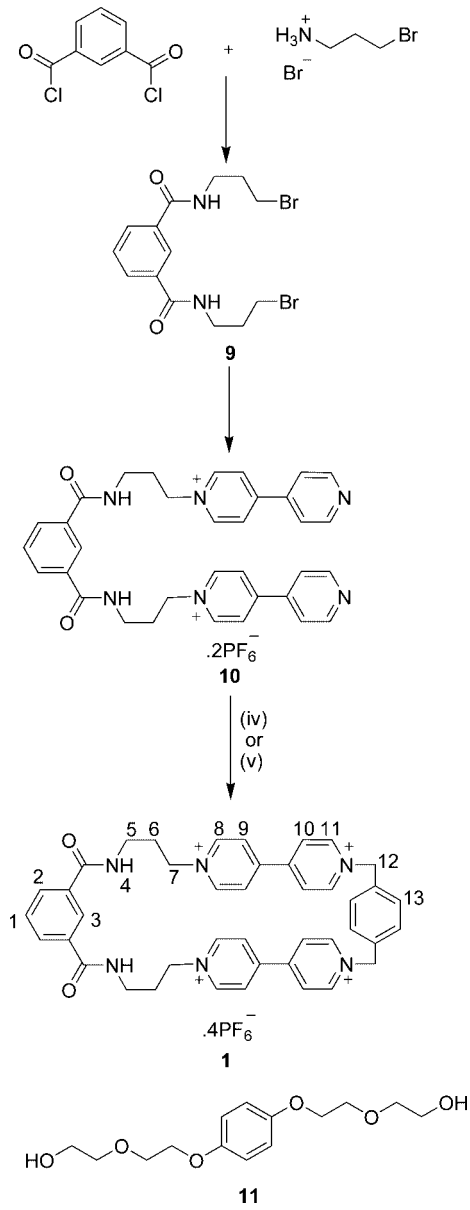


[a] Reagents and conditions: (i) $Et_3N$, $CH_2Cl_2$, room temperature, 18 h, 35%; (ii) 4,4′-bipyridine, $CH_3CN$, reflux, 24 h; (iii) $NH_4PF_6/H_2O$, 73%; (iv) 1,4-bis(bromomethyl)benzene, $CH_3CN$, reflux, 48 h, then $NH_4PF_6/H_2O$, 37%; (v) 1,4-bis(bromomethyl)benzene, **11**, $CH_3CN$, room temperature, 7 days, then $NH_4PF_6/H_2O$, 43%.

conditions to afford the target macrocycle **1** in 37% yield after silica gel column chromatography and anion exchange. A comparable yield of 43% was obtained by performing the reaction at room temperature using compound **11** to template the formation of the macrocycle.[25]

Single crystals of macrocycle **1** suitable for X-ray structure determination were grown by vapor diffusion of diisopropyl ether into a solution of the macrocycle in $CH_3CN$. In the solid state the macrocycle stacks in a head-to-head configuration with a $PF_6^-$ counteranion accommodated within the central cavity. The bipyridinium groups are orientated orthogonally to one another, while the isophthalamide carbonyl groups adopt a *syn*−*anti* conformation, with a weak intramolecular hydrogen-bonding interaction (O−C distance of 3.16 Å) between bipyridinium proton 8 and the oxygen atom of an amide group (Figure 2).

**Interpenetrative Binding Studies.** The propensity for macrocycle **1** to form pseudorotaxane assemblies with the unsubstituted indolocarbazole **12** and indolocarbazole derivatives **4**, **5**, and **8** was investigated.

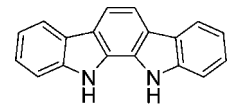


**12**

When the macrocycle was added to colorless solutions of the indolocarbazole compounds in $CH_3CN$, a strong pink/purple coloration was observed as a result of charge-transfer interactions between the HOMO of the bound indolocarbazole derivative and the LUMO of the macrocycle. The development of charge-transfer bands at 460−565 nm was monitored by UV−visible spectroscopy on titration of macrocycle **1** into solutions of the indolocarbazole compounds in $CH_3CN$ (Figure 3 and Figure S21, Supporting Information).

Association constants were determined by Specfit[26] analysis of the titration data using a 1:1 stoichiometric binding model (Table 1). The indolocarbazole compounds displayed binding affinities in the range $180 < K < 1000\ M^{-1}$ for the macrocycle in $CH_3CN$. Table 1 shows that the presence of polyether functional groups in the indolocarbazole enhances binding, as evidenced by the larger association constants for **4** and **8** as compared to **5** and **12**. The electrostatic stabilization of inclusion complexes of related tetracationic macrocycles by polyether substituents on the aromatic guest has been well-documented.[27,28] The observation that **4** forms a stronger pseudorotaxane association complex with macrocycle **1** than the more electron-rich derivative **5** suggests that favorable electrostatic effects are more important than charge-transfer interactions in contributing to the overall stability of the pseudorotaxane assembly.

Further evidence of pseudorotaxane formation was provided by $^1H$ NMR spectroscopy. The $^1H$ NMR spectra of macrocycle **1**, indolocarbazole **8**, and a 1:1 mixture of the two in $CD_3CN$ are shown in Figure 4. Interpenetration of the indolocarbazole guest results in desymmetrization of the bipyridinium environment and a significant splitting of the signals for protons 8, 9, 10, and 11. Upfield shifts in the signals for indolocarbazole aromatic protons a, b, c, and d are also observed as a result of favorable $\pi-\pi$ stacking and C−H$\cdots\pi$ interactions with the bipyridinium and *p*-phenylene groups of the macrocycle. The broadening of these resonances can be attributed to dynamic exchange effects. Dipolar couplings between protons 8 and a; 5,6 and b; and 3 and d were observed in the $^1H$ NMR ROESY spectrum of a 1:1 mixture of macrocycle **1** and indolocarbazole **8** in $CD_3CN$. Since these interactions have an $r^{-6}$ dependence, their existence is highly indicative of the close spacial proximity of the indolocarbazole motif to the macrocycle in solution and thus provides strong evidence of pseudorotaxane formation. Analogous results were obtained for indolocarbazole derivatives **4** and **5**.

(25) Anelli, P. L.; Ashton, P. R.; Ballardini, R.; Balzani, V.; Delgado, M.; Gandolfi, M. T.; Goodnow, T. T.; Kaifer, A. E.; Philp, D. *J. Am. Chem. Soc.* **1992**, *114*, 193–218.

(26) *SPECFIT, 2.02*; Spectrum Software Associates: Chapel Hill, NC.

(27) Anelli, P. L. *J. Am. Chem. Soc.* **1992**, *114*, 193–218.

(28) Castro, R.; Nixon, K. R.; Evanseck, J. D.; Kaifer, A. E. *J. Org. Chem.* **1996**, *61*, 7298–7303.

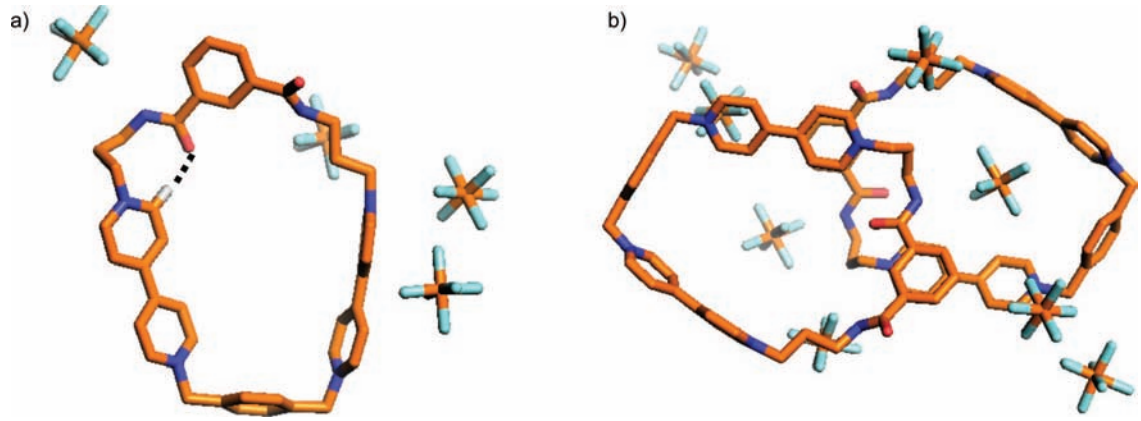


***Figure 2.*** Solid-state structure of macrocycle **1** (O, red; H, gray; C, orange; N, blue; P, orange; F, green). Solvent molecules and hydrogen atoms (except those involved in hydrogen bonding) have been omitted for clarity. Hydrogen bond represented as dashed line.

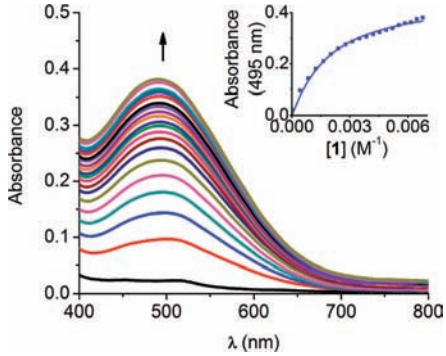


***Figure 3.*** Changes in the visible spectrum of a 0.65 mM solution of indolocarbazole **4** in $CH_3CN$ on addition of macrocycle **1** at 298 K. Inset: Change in the absorbance at 495 nm as a function of [macrocycle **1**] with calculated curve for $K = 630$ M$^{-1}$.

***Table 1.*** Stability Constants (M$^{-1}$) for 1:1 Complexes of Macrocycle **1** with Indolocarbazole Derivatives **4**, **5**, **8**, and **12** in $CH_3CN$ at 298 K and Absorption Maxima (nm) for the Charge-Transfer Bands

| indolocarbazole derivative | $\lambda_{max}$(CT band) | $K^a$ |
|---|---|---|
| **12** | 525 | 180 |
| **5** | 565 | 200 |
| **8** | 560 | 1000 |
| **4** | 495 | 630 |

[a] Errors <10%.

Increasing the solvent polarity was found to have a negative effect on binding, with no significant charge-transfer bands being observed in either $CH_3CN$:$H_2O$ (9:1 v/v) mixtures or DMSO. Small (<0.1 ppm) shifts in the indolocarbazole aromatic signals were observed by $^1$H NMR spectroscopy when indolocarbazole **4** was titrated against macrocycle **1** in DMSO-$d_6$, and a weak association constant of $K = 30$ M$^{-1}$ was calculated by WinEQNMR[29] analysis of the titration data. The observation that pseudorotaxane formation is suppressed in more polar solvents suggests that there is no significant solvophobic contribution toward binding for this system.[21,30]

A pseudorotaxane consisting of macrocycle **1** and the unsubstituted indolocarbazole **12** was obtained and characterized in the solid state. Red crystals suitable for X-ray diffraction

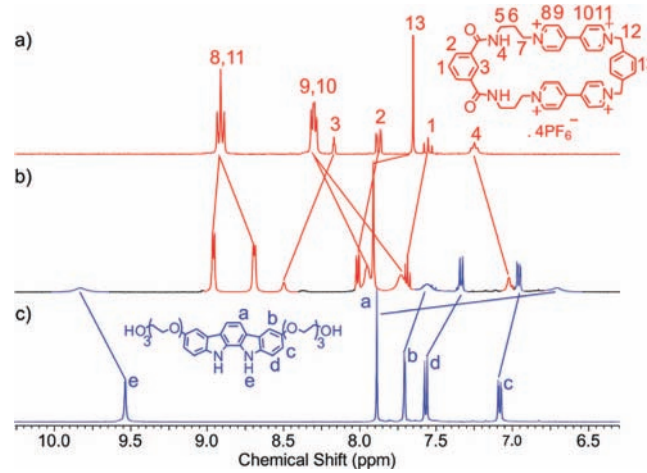


***Figure 4.*** Partial $^1$H NMR spectra of (a) macrocycle **1**, (b) a 1:1 mixture of macrocycle **1** and indolocarbazole **8**, and (c) indolocarbazole **8** in $CD_3CN$ at 293 K.

were grown by vapor diffusion of diisopropyl ether into a 1:1 solution of the two components in $CH_3CN$. The crystals were extremely small and weakly diffracting, and a synchrotron radiation source was necessary to determine the structure. The content of the asymmetric unit is shown in Figure 5. This essentially contains a pseudorotaxane unit and a free "host" **1** molecule. Two unencapsulated indolocarbazole molecules were found in the close proximity of each of the macrocycles. These indolocarbazole molecules interact with the bipyridinium groups of the host through $\pi-\pi$ stacking. The structure of the free macrocycle appears to be ruffled, considerably more so than the one discussed above (i.e., obtained in the absence of a guest), in which the bipyridinium groups are arranged orthogonally with respect to each other (Figure 2). The encapsulation of the indolocarbazole seems to lead to a more ordered structure for the host molecule. The encapsulated thread is oriented in a perpendicular fashion with respect to the free indolocarbazole molecule present in the proximity of a bipyridinium fragment. A multicomponent $\pi$-stacked system, bipyridinium−encapsulated indolocarbazole−bipyridinium−free indolocarbazole, is thus obtained in the solid state. The aromatic stacking distances relevant to the interpenetrated and non-interpenetrated guests appear to be within the expected range. The shortest of these interplanar distances (ca. 3.1 Å) was found between the best plane of the guest (within the pseudorotaxane component of this co-crystallite) placed in an offset position with respect to

(29) Hynes, M. J. *J. Chem. Soc., Dalton Trans.* **1993**, 311–312.
(30) Smithrud, D. B.; Diederich, F. *J. Am. Chem. Soc.* **1990**, *112*, 339–343.

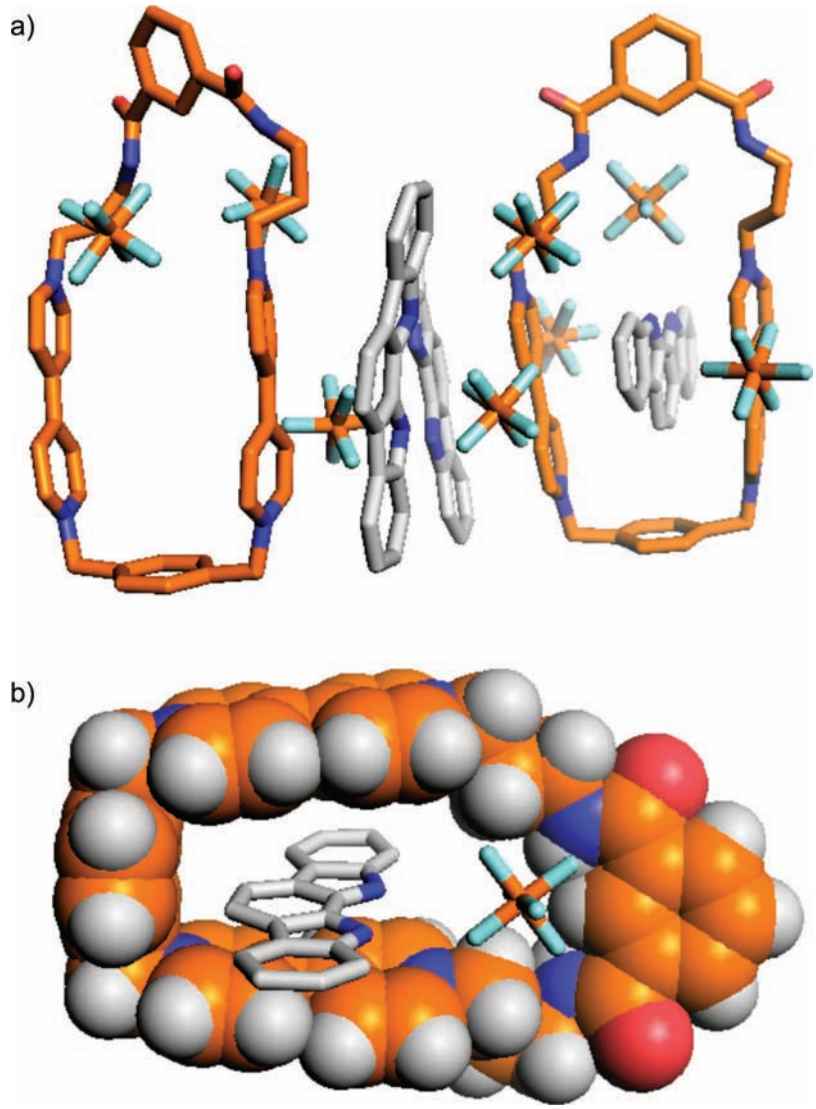


***Figure 5.*** X-ray structure of the pseudorotaxane: (a) content of the asymmetric unit and (b) space-filling model of the pseudorotaxane, also showing one of the associated $PF_6^-$ counterions. (Macrocycle **1**: O, red; H, gray; C, orange; N, blue; P, orange; F, green. Indolocarbazole **12**: C, gray; N, blue). Solvent molecules and hydrogen atoms (except those in the space-filling model) have been omitted for clarity.

the best plane of the host bipyridinium group containing N(5). The longest such distance was the one found between the free guest placed in proximity of the free host: the distance between the best plane of this non-interpenetrated guest and best plane of the bipyridinium group containing N(12) is ca. 3.85 Å. The most relevant aromatic stacking distances and corresponding labeling diagrams are included as Supporting Information. This multicomponent $\pi$-stacked arrangement appears to be further reinforced by a variety of close contacts involving the N−H groups of the thread and the host and the eight $PF_6^-$ counterions present. The free macrocycle encapsulates two of the $PF_6^-$ counterions, while the pseudorotaxane holds only one $PF_6^-$ inside the cavity. All of the bound $PF_6^-$ counterions are held in close proximity to the isophthalamide groups of the host molecules *via* short N−H···F contacts. All remaining $PF_6^-$ groups are involved in close contacts with the N−H groups of the free indolocarbazoles. In addition, there are a large number of disordered $CH_3CN$ and $H_2O$ molecules, some in close proximity to the macrocycle's cavity.

**[2]Rotaxane Synthesis.** Indolocarbazole derivative **4** was chosen as the precursor to the axle component of the rotaxane due to its relative ease of synthesis and oxidative stability compared to compounds **5** and **8**. Compound **4** was functionalized with sterically bulky stoppering groups to afford the stoppered axle component **16** using a dibutyltin dilaurate-catalyzed urethane formation reaction.[31] Isocyanate derivative **14** was prepared by treatment of the known compound **13** with triphosgene and $Et_3N$ in toluene. This was subsequently stirred at room temperature with indolocarbazole **4** and a catalytic amount of dibutyltin dilaurate in $CH_3CN$ for 60 h to afford compound **16** in 86% yield after column chromatography and recrystallization (Scheme 3).

In order to exploit the mildness and efficiency of this urethane stoppering reaction in [2]rotaxane synthesis, a 1:1 mixture of

(31) Huang, Y. L.; Hung, W. C.; Lai, C. C.; Liu, Y. H.; Peng, S. M.; Chiu, S. H. *Angew. Chem., Int. Ed.* **2007**, *46*, 6629–6633. Furusho, Y.; Sasabe, H.; Natsui, D.; Murakawa, K.; Takata, T.; Harada, T. *Bull. Chem. Soc. Jpn.* **2004**, *77*, 179–185. Furusho, Y.; Matsuyama, T.; Takata, T.; Moriuchi, T.; Hirao, T. *Tetrahedron Lett.* **2004**, *45*, 9593–9597.

***Scheme 3.*** Synthesis of [2]Rotaxane **15**[a]

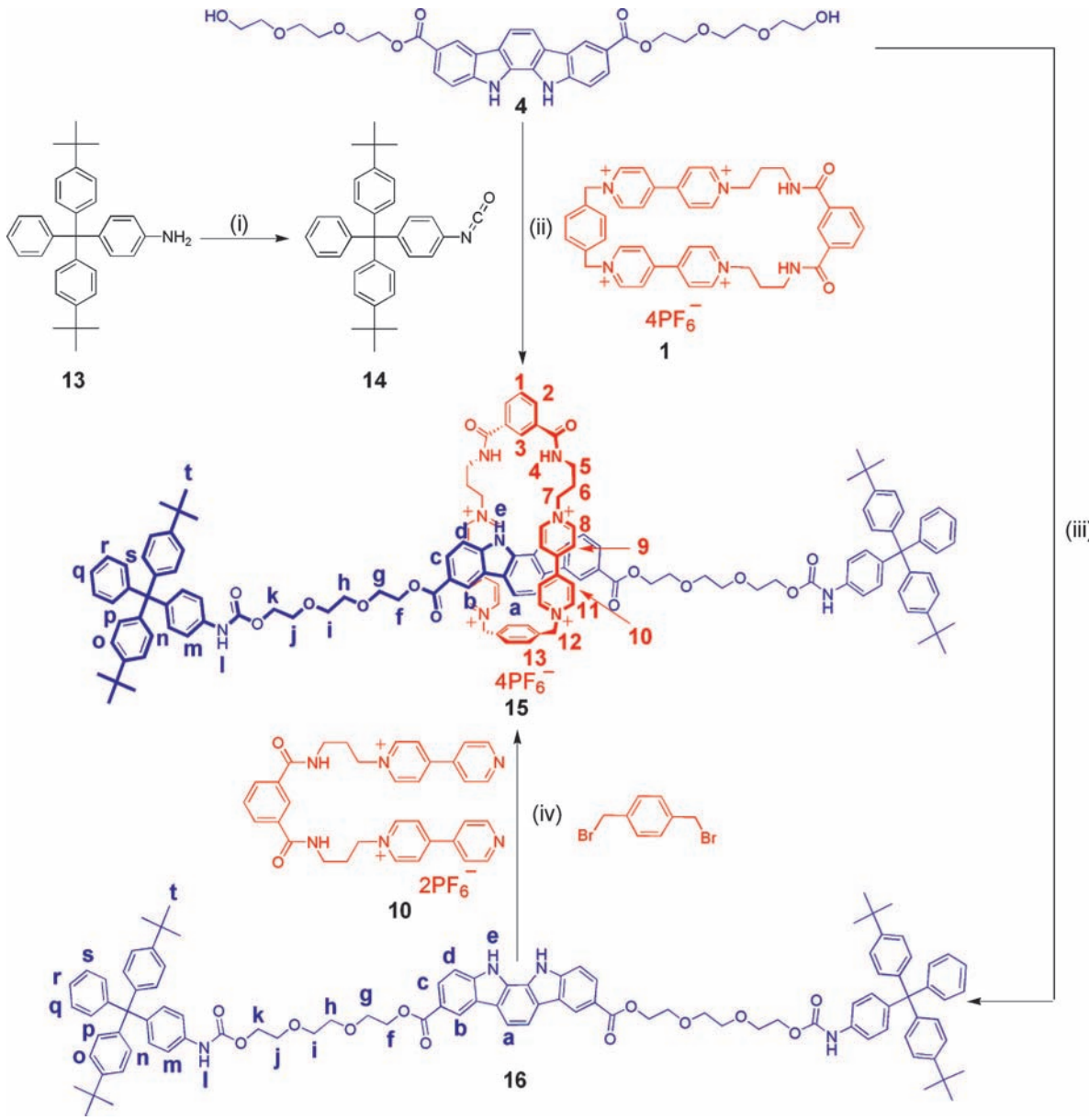


[a] Reagents and conditions: (i) triphosgene, $Et_3N$, toluene, reflux, 4 h; (ii) di-*n*-butyltin dilaurate, $CH_3CN$, room temperature, 60 h, 19% or di-*n*-butyltin dilaurate, TBACl, $CH_3CN$, room temperature, 60 h, 21%; (iii) **14**, di-*n*-butyltin dilaurate, $CH_3CN$, 48 h, 86%, (iv) $CH_3CN$, room temperature, 10 days, then excess $NH_4PF_6$ in $(CH_3)_2CO$, 10%.

indolocarbazole **4** and macrocycle **1** was stirred with an excess of the isocyanate-functionalized stopper **14** in the presence of the tin catalyst in $CH_3CN$ under the same conditions. After silica gel column chromatography, the [2]rotaxane **15** was isolated as a purple solid in 19% yield. When the reaction was carried out in the presence of 1 equiv of tetrabutylammonium (TBA) chloride, a comparable yield of 21% was obtained, suggesting that the chloride anion neither significantly templates nor inhibits pseudorotaxane assembly.

Compound **15** was also successfully synthesized *via* reaction of macrocycle precursor **10** with 1,4-bis(bromomethyl)benzene in the presence of stoppered axle **16** in $CH_3CN$ at room temperature. However, the [2]rotaxane was isolated from this clipping reaction in a reduced yield of 10% yield after column chromatography and ion exchange. It is noteworthy that, based on a comparison of the yields obtained for the stoppering and clipping reactions, the bromide anions generated during the clipping reaction do not appear to play a significant templating role. The higher rotaxane yield associated with the stoppering methodology suggests a thermodynamic preference by the indolocarbazole axle for the tetracationic macrocycle **1** than for the macrocycle's acyclic precursors. This result is consistent with previous work by Stoddart and co-workers on related $\pi$-donor−acceptor systems.[32]

(32) Dichtel, W. R.; Miljanic, O. S.; Spruell, J. M.; Heath, J. R.; Stoddart, J. F. *J. Am. Chem. Soc.* **2006**, *128*, 10388–10390. Braunschweig, A. B.; Dichtel, W. R.; Miljanic, O. S.; Olson, M. A.; Spruell, J. M.; Khan, S. I.; Heath, J. R.; Stoddart, J. F. *Chem.-Asian J.* **2007**, *2*, 634–647.

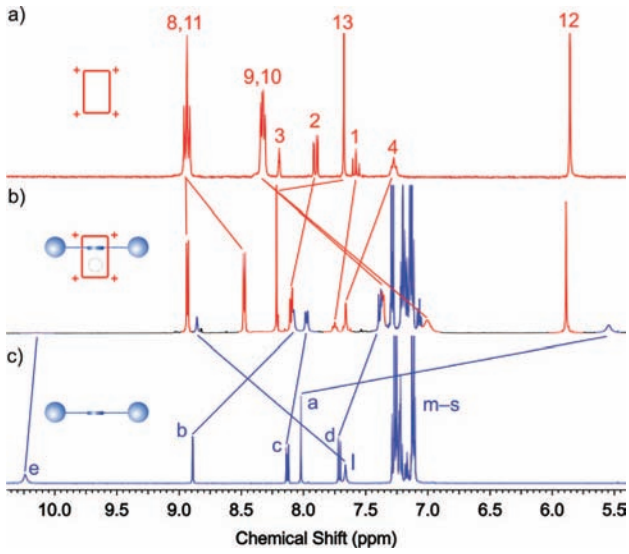


***Figure 6.*** Partial $^1$H NMR spectra of (a) macrocycle **1**, (b) [2]rotaxane **15**, and (c) stoppered axle **16** in $CD_3CN$ at 293 K.

The [2]rotaxane was characterized by NMR spectroscopy, electrospray mass spectrometry, and UV−visible spectroscopy. The $^1$H NMR spectrum of rotaxane **15** in $CD_3CN$ is compared with those of stoppered thread **16** and macrocycle **1** in Figure 6. The spectrum of the rotaxane was fully assigned with the aid of COSY, HMBC, and HSQC techniques. The indolocarbazole aromatic protons a−d and bipyridinium protons 8 and 9 resonate at higher field in the spectrum of the rotaxane than in those of the free stoppered axle and macrocycle as a result of shielding by favorable $\pi-\pi$ stacking interactions. The particularly large upfield shift observed for proton a ($\Delta\delta \approx 2.5$ ppm) suggests the existence of edge-to-face interactions between this proton and the *p*-phenylene group of the macrocycle. Large splittings in the signals for bipyridinium protons 8−11 are also observed due to desymmetrization by the interpenetrated indolocarbazole axle.

The $^1$H NMR ROESY spectrum of compound **15** shows several through-space couplings between the two interlocked components of the rotaxane (Figure 7). Importantly, the existence of a strong dipolar interaction between proton a and proton 13, with weaker interactions between proton a and bipyridinium protons 10 and 11, implies that the indolo-NH groups point toward the isophthalamide cleft, defining a hydrogen-bond-donating binding pocket. This orientation is consistent with that observed in the solid-state structure of the pseudorotaxane described above (Figure 5). NOEs between protons f−k and bipyridinium protons 10, 11, and 13 indicate the spacial proximity of the indolocarbazole polyether groups to the macrocycle, which reinforces the importance of the electrostatic stabilization afforded by these groups.

Further evidence for the interlocked structure of the [2]rotaxane was provided by electrospray mass spectrometry, which revealed peaks at $m/z$ = 2652.79, 2506.83, and 2361.89 corresponding to $[M - PF_6]^+$, $[M - 2PF_6]^+$, and $[M - 3PF_6]^+$ respectively (Figure S19, Supporting Information).[33]

The UV−visible spectrum of the rotaxane in $CH_3CN$ shows a strong absorbance ($\epsilon$ = 55 000 $M^{-1}cm^{-1}$) at 260 nm arising from aromatic $\pi-\pi^*$ transitions and a weaker absorbance ($\epsilon$ = 890 $M^{-1}$ $cm^{-1}$) at 498 nm due to charge-transfer interactions between the indolocarbazole and bipyridinium groups. Comparison of the visible spectrum of the rotaxane with that of a 1:1 mixture of indolocarbazole **4** and macrocycle **1** in $CH_3CN$ at the same concentration shows that, as expected, the intensity of the charge-transfer band is considerably greater for the interlocked compound (Figure 8).

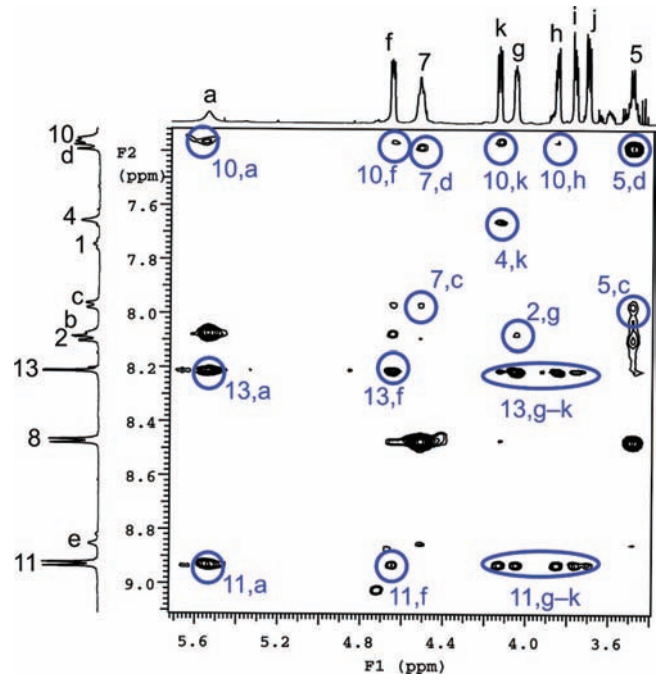


***Figure 7.*** Section of the $^1$H NMR ROESY spectrum of [2]rotaxane **15** in $CD_3CN$ at 293 K.

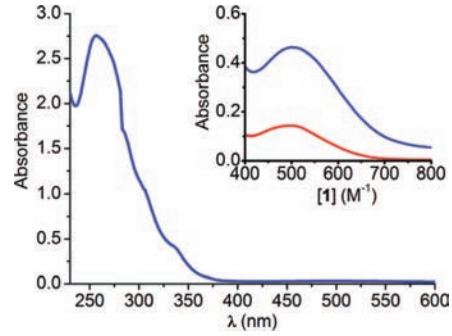


***Figure 8.*** UV−visible spectrum of [2]rotaxane **15** (0.05 mM) in $CH_3CN$ at 298 K. Inset: Visible spectra of [2]rotaxane **15** (0.5 mM, blue line) and a 1:1 mixture of indolocarbazole **4** and macrocycle **1** (0.5 mM, red line) in $CH_3CN$ at 298 K.

**Anion-Binding Studies.** The anion-binding properties of indolocarbazole **4**, macrocycle **1**, and rotaxane **15** were probed by $^1$H NMR spectroscopic titration experiments. The titration experiments were carried out in DMSO-$d_6$, as the halide salts of macrocycle **1** and [2]rotaxane **15** were found to precipitate from less polar solvent systems.

(33) The mass spectrum of [2]rotaxane **15** is characteristic of those reported for interlocked structures incorporating tetracationic bipyridinium macrocycles. See for example: Amabilino, D. B.; Ashton, P. R.; Brown, C. L.; Cordova, E.; Godinez, L. A.; Goodnow, T. T.; Kaifer, A. E.; Newton, S. P.; Pietraszkiewicz, M. *J. Am. Chem. Soc.* **1995**, *117*, 1271–1293. Stoddart, J. F.; Williams, D. J.; Amabilino, D. B.; Anelli, P.-L.; Ashton, P. R.; Brown, G. R.; Cordova, E.; Godinez, L. A.; Hayes, W. *J. Am. Chem. Soc.* **1995**, *117*, 11142–11170. Maxwell, J.; Gunter, M. J.; Jeynes, T. P.; Turner, P. *Eur. J. Org. Chem.* **2004**, *2004*, 193–208.

***Table 2.*** Stability Constants ($M^{-1}$) for 1:1 Complexes of Macrocycle **1**, Indolocarbazole **4**, and [2]Rotaxane **15** with Various Anions in DMSO-$d_6$ at 293 K

| | 1 | | 4 | | 15 | |
|---|---|---|---|---|---|---|
| anion | $\Delta\delta$ | $K$ | $\Delta\delta$ | $K$ | $\Delta\delta$ | $K$ |
| $Cl^-$ | 1.03 | 380[a] | 0.43 | 120[a] | 0.39 | 3000[a] |
| $Br^-$ | 0.23 | 150[a] | 0.07 | 70[a] | 0.16 | 850[a] |
| $I^-$ | 0.04 | 60[a] | 0.06 | <50 | 0.03 | 90[a] |
| $NO_3^-$ | 0.02 | 40[a] | – | –[b] | 0.01 | 20[a] |

[a] Errors <10%. [b] No evidence of association. $\Delta\delta$: changes in the induced chemical shifts (ppm) of the CH (compounds **1** and **15**, proton 3) or NH (compound **4**, proton e) resonances after addition of 10 equiv of the anion. All anions were added as their TBA salts.

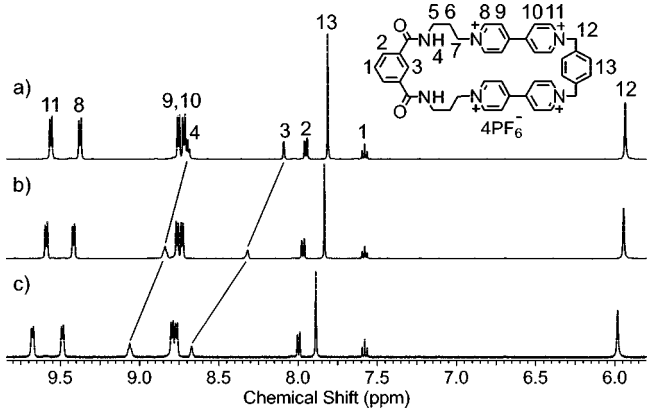


***Figure 9.*** Partial $^1$H NMR spectra of macrocycle **1** in the presence of (a) 0, (b) 1, and (c) 5 equiv of TBACl in DMSO-$d_6$ at 293 K.

**Indolocarbazole 4.** Simple indolocarbazole derivatives are known to recognize anionic guests through hydrogen-bonding interactions mediated by their preorganized pyrrole N−H groups.[11,19] As expected, addition of the TBA salts of $Cl^-$, $Br^-$, and $I^-$ to indolocarbazole **4** in DMSO-$d_6$ induced downfield shifts in the N−H proton signals due to polarization of the N−H bonds upon anion complexation (Figures S22 and S23a, Supporting Information). Negligible perturbations in the spectrum were observed on addition of $TBANO_3$, which suggests that the trigonal $NO_3^-$ anion is not bound by the indolocarbazole receptor. Association constants for $Cl^-$, $Br^-$, and $I^-$ were determined by fitting the changes in the chemical shift of the N−H proton e to a 1:1 binding model using WinEQNMR[29] software. Both the strength of anion association and the magnitude of the induced chemical shifts were observed to increase with increasing hydrogen-bond-acceptor ability of the anion ($I^- < Br^- < Cl^-$). However, in this competitive solvent system, association was relatively weak ($K \leq 120\ M^{-1}$) for all anions studied (Table 2).

**Macrocycle 1.** Similarly, addition of anions as their TBA salts to macrocycle **1** in DMSO-$d_6$ induced perturbations in isophthalamide protons 3 and 4 and in protons 5−13 (Figure 9). The largest shifts were observed for isophthalamide protons 3 and 4, which suggests that the anions are predominantly bound in the vicinity of the isophthalamide cleft by a combination of hydrogen-bonding and electrostatic interactions. Association constants were obtained by monitoring the changes in the chemical shift of proton 3 (Figure S23b, Supporting Information) and analyzing the resulting titration curves using WinEQNMR[29] software (Table 2). For all anions a good fit was achieved using 1:1 binding models. The strength of anion association was observed to increase in the order $NO_3^- < I^- < Br^- < Cl^-$. This trend is consistent with those reported for simple acyclic isophthalamide derivatives and is thought to reflect the size and shape complementarity of the isophthalamide-binding cleft to the $Cl^-$ anion.[2,3]

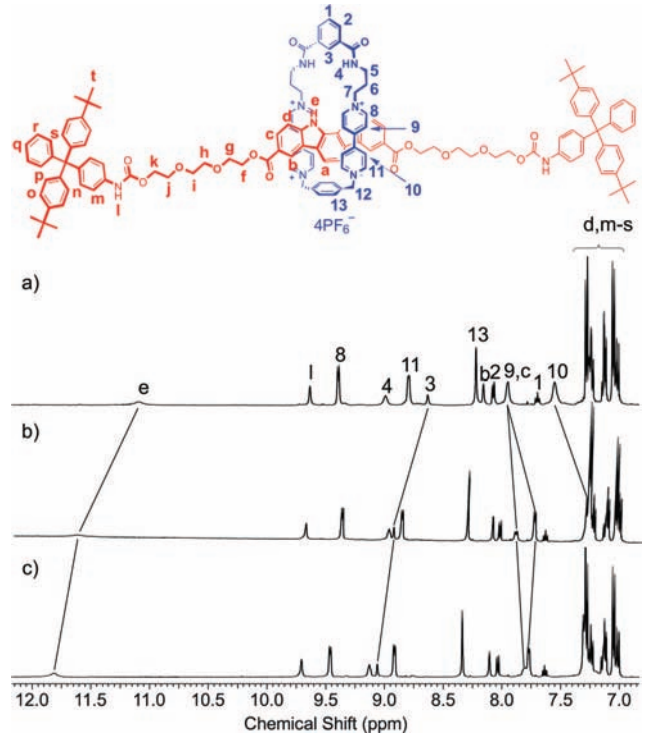


***Figure 10.*** Partial $^1$H NMR spectra of [2]rotaxane **15** in the presence of (a) 0, (b) 1, and (c) 5 equiv of TBACl in DMSO-$d_6$ at 293 K.

Unfortunately, addition of the TBA salts of $AcO^-$, $H_2PO_4^-$, $F^-$, and $SO_4^{2-}$ resulted in rapid chemical decomposition of macrocycle **1**. Addition of these anions to degassed solutions of the macrocycle caused the solutions to adopt the characteristic blue color of the viologen radical cation. Upon exposure to air the solutions decolorized within seconds, but when kept under nitrogen the blue color persisted indefinitely and gradually intensified over time. This suggests that decomposition is preceded by a one-electron reduction of the bipyridinium groups, presumably as a result of charge transfer from the anions.[34] Viologen radical cations are known to reduce molecular oxygen to form hydroxide,[35] and nucleophilic attack by this species adjacent to the bipyridinium groups could explain the decomposition of the macrocycle in aerated solutions.

**[2]Rotaxane 15.** Addition of anions as their TBA salts to a solution of [2]rotaxane **15** in DMSO-$d_6$ induced downfield shifts of the indolocarbazole N−H proton e and macrocycle isophthalamide proton 3 (Figure 10). Monitoring the downfield shift in proton 3 upon anion addition allowed stability constants to be determined (Figure S23c, Supporting Information). It is noteworthy that there is a marked nearly 10-fold and over 5-fold increase in the rotaxane's binding affinities for $Cl^-$ and $Br^-$, respectively, over those of macrocycle **1** (Table 2). This highlights the cooperative recognition of the halide anions by favorable hydrogen-bond donation from both axle indolocarbazole N−H (proton e) and macrocycle isophthalamide (protons 3 and 4) components of the rotaxane. Indeed, the observed

(34) Dickson, S. J.; Wallace, E. V. B.; Swinburne, A. N.; Paterson, M. J.; Lloyd, G. O.; Beeby, A.; Belcher, W. J.; Steed, J. W. *New J. Chem.* **2008**, *32*, 786–789.
(35) Bird, C. L.; Kuhn, A. T. *Chem. Soc. Rev.* **1981**, *10*, 49–82.

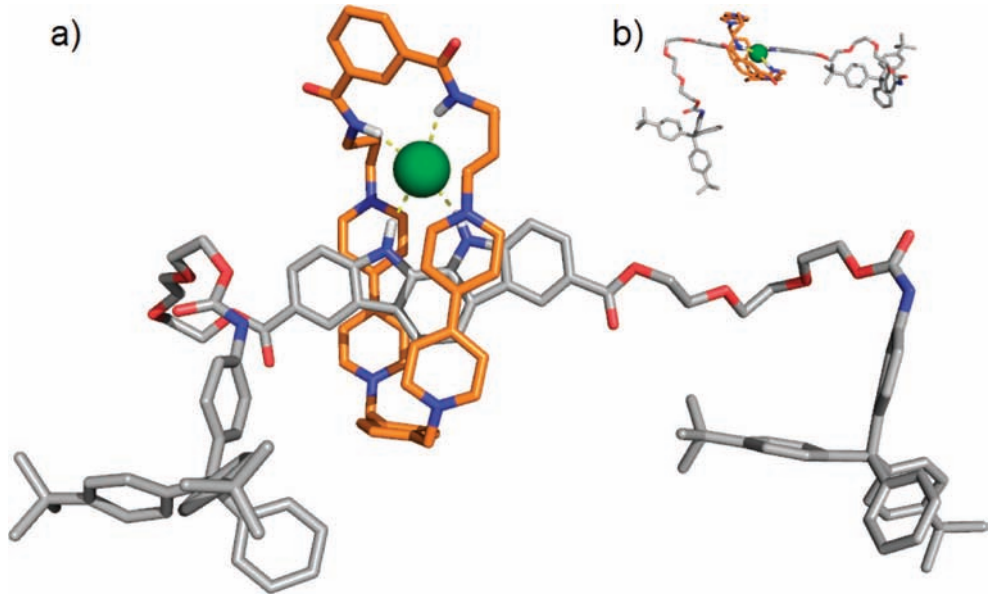


***Figure 11.*** MD snapshot of the 1:1 association between $Cl^-$ (green sphere) and the [2]rotaxane **15**: (a) side view and (b) top view. Solvent molecules, counteranions, and C−H hydrogens have been omitted for clarity; hydrogen bonds are presented as yellow dashes.

downfield shift of proton 3 upon addition of anions was comparatively smaller for [2]rotaxane **15** than for macrocycle **1**, which may be a result of the anions being slightly polarized away from the isophthalamide group by additional hydrogen-bonding interactions with the indolocarbazole N−H protons (e) in the rotaxane. The rotaxane amplifies the selectivity of macrocycle **1** and indolocarbazole **4** for $Cl^-$ and $Br^-$ over $I^-$ and $NO_3^-$, which indicates that the unique interlocked binding cavity of [2]rotaxane **15** is of an optimal size and shape complementarity to these halide anions.

As in the case of macrocycle **1**, the rotaxane was decomposed by addition of the TBA salts of $F^-$, $AcO^-$, $SO_4^{2-}$, and $H_2PO_4^-$, which prohibited the determination of association constants for these anions by $^1H$ NMR spectroscopy.

**Molecular Modeling Studies.** Computational molecular dynamics (MD) simulations were undertaken to further elucidate the structural nature of the association process between the anions $Cl^-$, $Br^-$, $I^-$, and $NO_3^-$ and the [2]rotaxane **15**.

Conventional 10 ns long MD simulations were performed on the 1:1 complexes of **15** with the various anions immersed in a cubic box of explicit DMSO molecules (a detailed description of the generation of the starting structures may be found below). The binding arrangement of **15** to halide anions is illustrated in Figure 11 with a snapshot taken from the MD simulation with $Cl^-$. The indolocarbazole entity is $\pi-\pi$ stacked between the two bipyridinium fragments of the macrocycle, as found in the crystal structure of pseudorotaxane described above (Figure 5). The $Cl^-$ anion is hydrogen-bonded to the N−H binding sites of the isophthalamide cleft and the indolocarbazole thread.

By monitoring the isophthalamide and indolocarbazole N−H···X (X = $Cl^-$, $Br^-$, $I^-$, and $NO_3^-$) distances, some insights into the selectivity trends and preferential binding location of the anions to the [2]rotaxane were possible. The measured N−H···X distances are reflected in the probability distribution functions (PDFs) of the corresponding time series, presented as Supporting Information. Close analyses of the isophthalamide N−H···X distance PDF (Figure S24) revealed both $Cl^-$ and $Br^-$ to be preferentially located at 2.5 Å from the N−H binding sites, whereas $I^-$ is located at 2.9 Å from the N−H groups. Similarly, the PDFs of the indolocarbazole N−H···X distances (Figure S25) indicate $Cl^-$, $Br^-$ and $I^-$ to be mostly sited at 2.1, 2.3, and 2.5 Å from the binding sites. However, the slightly shorter indolocarbazole N−H···X distances, along with the sharper peaks of the corresponding PDF curves, clearly suggest that the monatomic anions establish stronger interactions with the indolocarbazole entity than with the isophthalamide moiety. This is clearly evident in the N−H···X average distances and corresponding standard deviations, listed in Table 3. As can be seen, the indolocarbazole N−H···X distances are shorter and less broadened in comparison to the isophthalamide N−H···X lengths.

***Table 3.*** Average N−H···X Distances (Å) between X (X = $Cl^-$, $Br^-$, $I^-$, and $NO_3^-$) and the Hydrogen Atoms of the Indolocarbazole and Isophthalamide N−H Binding Sites

| anion | isophthalamide[a] | | indolocarbazole[a] | |
|---|---|---|---|---|
| $Cl^-$ | $2.5_6 \pm 0.2_3$ | $2.5_0 \pm 0.2_3$ | $2.2_4 \pm 0.1_8$ | $2.2_5 \pm 0.1_6$ |
| | (*1.96*, **4.24**) | (*1.93*, **4.63**) | (*1.81*, **5.14**) | (*1.86*, **3.79**) |
| $Br^-$ | $2.5_8 \pm 0.2_2$ | $2.5_8 \pm 0.2_2$ | $2.2_9 \pm 0.1_8$ | $2.2_8 \pm 0.1_6$ |
| | (*1.96*, **4.03**) | (*1.98*, **4.13**) | (*1.91*, **4.39**) | (*1.91*, **3.88**) |
| $I^-$ | $3.5_2 \pm 1.3_8$ | $3.6_0 \pm 1.4_0$ | $2.8_5 \pm 0.6_2$ | $3.3_1 \pm 1.2_6$ |
| | (*2.31*, **8.97**) | (*2.32*, **8.75**) | (*2.14*, **6.11**) | (*2.18*, **8.12**) |
| $NO_3^-$ | $3.2_9 \pm 0.9_0$ | $3.1_1 \pm 0.7_5$ | $2.7_4 \pm 0.8_0$ | $2.7_9 \pm 0.7_7$ |
| | (*1.63*, **6.16**) | (*1.58*, **5.67**) | (*1.55*, **5.67**) | (*1.57*, **5.27**) |
| | $3.3_1 \pm 0.8_1$ | $2.9_9 \pm 0.7_4$ | $2.8_7 \pm 0.8_0$ | $2.8_8 \pm 0.8_0$ |
| | (*1.65*, **6.10**) | (*1.64*, **5.30**) | (*1.56*, **5.56**) | (*1.55*, **4.87**) |
| | $3.3_5 \pm 0.8_1$ | $3.0_9 \pm 0.8_1$ | $2.9_0 \pm 0.7_8$ | $2.8_2 \pm 0.8_3$ |
| | (*1.62*, **6.06**) | (*1.63*, **5.53**) | (*1.55*, **5.10**) | (*1.52*, **5.77**) |

[a] Average ± standard deviation (*minimum*, **maximum**), $N = 50\,000$.

Considering that shorter N−H···X distances and sharper distance PDFs imply stronger interactions and, consequently, higher association constants, these are expected to decrease when going from $Cl^-$ to $Br^-$ and to $I^-$. In addition, and from the indolocarbazole N−H···$I^-$ distance PDF, several maxima are encountered at about 4.3 and 6.1 Å (at 6.7 Å in the isophthalamide N−H···$I^-$ PDF), indicating that $I^-$ is momentarily located outside the rotaxane binding pocket. In fact, from the time evolution of the several N−H···$I^-$ distances, $I^-$ can be encountered interacting with the indolocarbazole binding sites

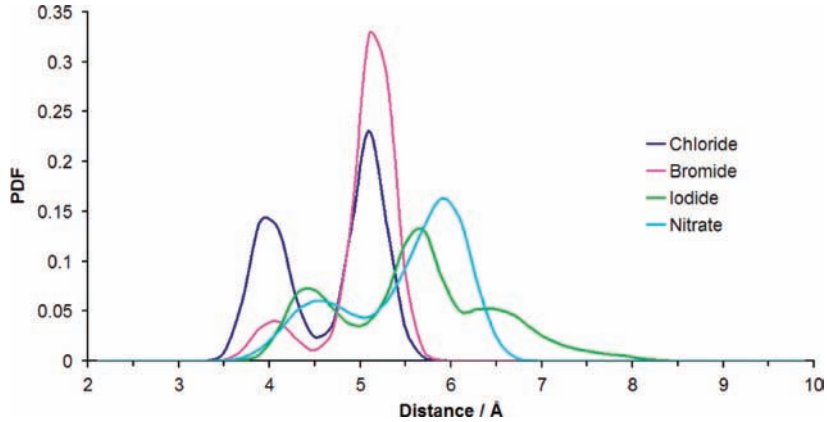


***Figure 12.*** PDF of the *indolocarbazole···isophthalamide* distance in the 1:1 complexes of **15** with the various anions ($Cl^-$, $Br^-$, $I^-$, and $NO_3^-$). The distance is the separation between the centers of mass defined by the nitrogen atoms of the indolocarbazole and isophthalamide moieties (see Figure S27, Supporting Information).

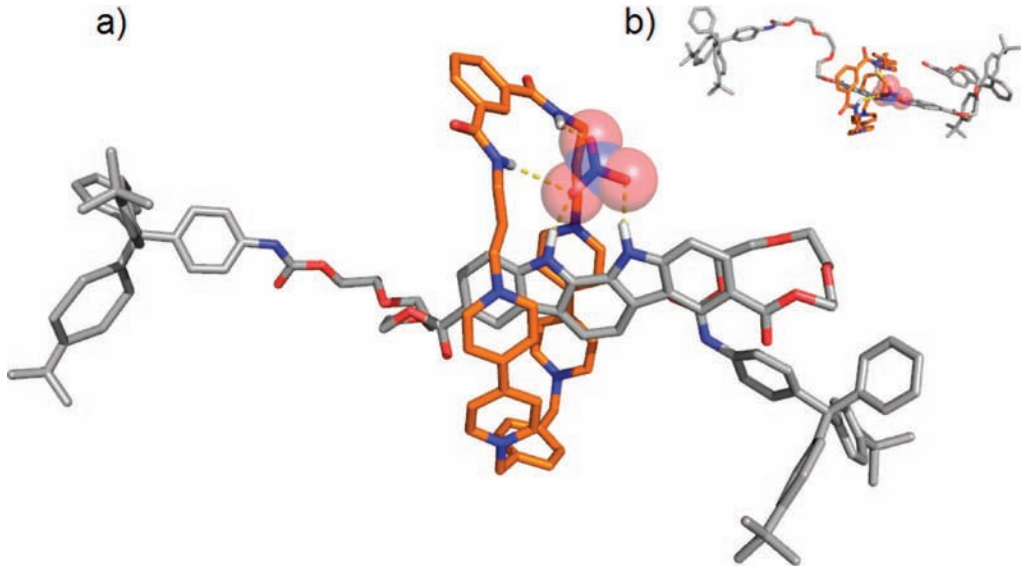


***Figure 13.*** MD snapshot of the 1:1 association between $NO_3^-$ (blue and red spheres) and the [2]rotaxane **15**: (a) side view and (b) top view. Details as in Figure 11.

while located away from the isophthalamide cleft, and *vice versa*. Furthermore, the distances between the indolocarbazole and isophthalamide N−H binding sites shift toward longer values with increasing anion size, reaching the longest values when the anion is either $I^-$ or $NO_3^-$. The two moieties are closest to each other when the interaction is mediated by $Cl^-$, as clearly shown in Figure 12.

Concerning the association of $NO_3^-$ to **15** (Figure 13), the wide band presented by the isophthalamide N−H···O−$NO_2^-$ PDF indicates the anion to be loosely bound to the N−H binding sites as a consequence of the bigger anionic size and the smaller negative charge distribution around the nitrate oxygen atoms. Additionally, as can be seen from the distance−time series at a given instant, the nitrate oxygens interacting with a given N−H binding site quickly exchange at the nanosecond time scale, leading to longer average N−H···O distances with large standard deviations (Table 3). However, again, the indolocarbazole N−H···O−$NO_2^-$ distance PDF presents sharper peaks relative to the isophthalamide one, indicating $NO_3^-$ to be preferentially and more tightly associated to the indolocarbazole binding sites. The presence of $NO_3^-$ pushes away the indolocarbazole and isophthalamide moieties in order to simultaneously allow interactions with both binding sites, leaving, however, part of the anion exposed to the solvent, as can been seen from Figures 12 and 13.

Succinctly, the results suggest that the interlocked binding pocket of [2]rotaxane **15** fulfills the requirements for the interaction with $Cl^-$ and $Br^-$ but not with bigger anions such as $I^-$ and $NO_3^-$, which have lower negative charge densities. The latter anions seem to push away both binding sites, leaving the isophthalamide N−H binding sites momentarily exposed to the solvent while solely interacting with the indolocarbazole moiety. The interaction of **15** with $Cl^-$ and $Br^-$ is thus characterized by higher association constants, in contrast to $I^-$ and $NO_3^-$. This conclusion is in total agreement with the experimental binding data reported in Table 2.

Validation of the above structural findings and halide association constant trends of [2]rotaxane **15** was made by performing thermodynamic integration calculations. Alchemic mutations of $Cl^-$ to $Br^-$ and $Br^-$ to $I^-$ were performed in explicit DMSO both in the presence and in the absence of the rotaxane, thus yielding the relative association free energies ($\Delta\Delta G$) of the anions to **15**. The results, which are summarized in Table 4, indicate that the association constants decrease with increasing

***Table 4.*** Relative Association Free Energies ($\Delta\Delta G$) and Corresponding Entropic and Enthalpic ($\Delta\Delta H$) Components ($T\Delta\Delta S$) of [2]Rotaxane **15** to $Cl^-$, $Br^-$, and $I^-$, As Obtained from Thermodynamic Integration Calculations at 300 K

| component (kcal mol$^{-1}$) | $Cl^- \rightarrow Br^-$ | $Br^- \rightarrow I^-$ |
|---|---|---|
| $\Delta\Delta H$ | 1.36 | 9.36 |
| $T\Delta\Delta S$ | 0.33 | 0.09 |
| $\Delta\Delta G$ | 1.03 | 9.27 |
| $\Delta\Delta G_{exp}$[a] | 0.73 | 1.31 |

[a] Experimental values ($\Delta\Delta G_{exp}$) are presented for comparison purposes.

anion size (i.e., when going from $Cl^-$ to $Br^-$ and to $I^-$) and, consequently, with decreasing anion charge density. In both transformations ($Cl^- \rightarrow Br^-$ and $Br^- \rightarrow I^-$), the contributions to the relative association free energies are essentially enthalpic and negligibly entropic ($T\Delta\Delta S$), although the enthalpic term is overestimated in the bromide-to-iodide mutation. However, it is worth noting that the calculated solvation free energies, obtained from the annihilation of the free anions in DMSO, are close to the experimental ones (Table S1, Supporting Information) and that the largest discrepancy found in the solvation $\Delta G$ of iodide is of only 1.5 kcal mol$^{-1}$. In other words, the reasonable agreement between experimental and calculated data suggests that the van der Waals parameters used are the appropriate ones, which validates the reported free energy calculations. Thus, the overall results are in total agreement with the experimentally determined association constants presented in Table 2, and clearly suggest the selectivity trend to be anion size dependent.

## Conclusion

The design and synthesis of the first indolocarbazole-containing interlocked structure has been achieved. The novel [2]rotaxane comprises an indolocarbazole-containing axle component and a new isophthalamide-functionalized macrocycle. This interlocked host structure has been shown to exhibit enhanced selectivity for chloride and bromide anions compared to the individual axle and macrocycle components. The rotaxane's affinity for chloride, bromide, iodide, and nitrate anions was shown by $^1$H NMR spectroscopy to decrease with increasing anion radius and decreasing charge density. Molecular dynamics simulations and thermodynamic integration calculations indicated that anion association is an enthalpically driven process mediated by hydrogen-bond donation from the indolocarbazole N−H and macrocycle isophthalamide protons. The computational studies suggested that, while chloride and bromide anions are of the correct size to interact cooperatively with both components, the larger iodide and nitrate anions are unable to fully penetrate the interlocked binding cavity. As a result, these anions remain more loosely associated with the rotaxane, tending to interact solely with the indolocarbazole N−H protons. Thus, the rotaxane's selectivity for chloride and bromide anions was shown to result from the optimal size-complementarity of its unique topologically constrained binding cavity to the smaller halide anions. Inspired by the very promising anion recognition properties exhibited by this first example of an indolocarbazole rotaxane, we are continuing the incorporation of the indolocarbazole motif into mechanically bonded host structures in our laboratories.

## Experimental Details

**General Considerations.** All solvents and reagents were purchased from commercial suppliers and used as received unless otherwise stated. Dry solvents were obtained by purging with nitrogen and then passing through an MBraun MPSP-800 column. $H_2O$ was deionized and microfiltered using a Milli-Q Millipore machine. $Et_3N$ was distilled and stored over KOH. TBA salts were stored in a vacuum desiccator containing phosphorus pentoxide prior to use. $^1$H, $^{13}$C, $^{19}$F, and $^{31}$P NMR spectra were recorded on a Varian Mercury-VX 300, a Varian Unity Plus 500, or a Bruker AVII500 instrument with cryoprobe at 293 K. Chemical shifts are quoted in parts per million relative to the residual solvent peak. Mass spectra were obtained using a Micromass GCT (EI), a Micromass LCT (ESMS), or a MALDI Micro MX instrument. Electronic absorption spectra were recorded on a Shimadzu UV-2401PC spectrophotometer. Microwave reactions were carried our using a Biotage Initiator 2.0 microwave. Melting points were recorded on a Gallenkamp capillary melting point apparatus and are uncorrected. Elemental analysis was carried out by the service at London Metropolitan University.

2-(2-(2-Hydroxyethoxy)ethoxy)ethyl 4-methylbenzenesulfonate (**7**),[36] 2,2′-(2,2′-(1,4-phenylenebis(oxy))bis(ethane-2,1-diyl))bis(oxy) diethanol (**11**),[27] indolo[2,3-*a*]carbazole (**12**),[37] and 4-(bis(4-*tert*-butylphenyl)(phenyl)methyl)aniline (**13**)[24] were prepared according to reported procedures.

**Dibutyl 11,12-Dihydroindolo[2,3-*a*]carbazole-3,8-dicarboxylate (2).** 1,2-Cyclohexanedione (0.56 g, 5.0 mmol) and 4-hydrazinebenzoic acid (1.7 g, 11 mmol) were suspended in *n*-butanol (100 mL), and concentrated $H_2SO_4$(aq) (1 mL) was added dropwise *via* syringe. The mixture was heated to reflux for 60 h and then cooled to room temperature and left to stand for 18 h. The resulting yellow precipitate was collected by filtration and consecutively washed with MeOH (3 × 5 mL), $H_2O$ (5 × 40 mL), and MeOH (2 × 20 mL). The solid was then dissolved in DMF (30 mL), and 10% Pd/C (0.16 g, ∼10% by weight) was added. The mixture was heated to reflux under an atmosphere of $N_2$ for 24 h and then filtered to remove the Pd/C, which was washed with hot DMF (3 × 10 mL). The combined filtrate and DMF washings were concentrated *in vacuo* to a volume of 20 mL, and $H_2O$ (100 mL) was added to precipitate the product. This was collected by filtration, washed with $H_2O$ (2 × 20 mL) followed by MeOH (5 mL), and dried under high vacuum to yield the product as a white solid (1.5 g, 68%): mp >300 °C; $^1$H NMR (500 MHz, DMSO-$d_6$) $\delta$ 11.66 (s, 2H, N*H*), 8.88 (d, $^4J$ = 1.5 Hz, 2H, Ar*H*), 8.15 (s, 2H, Ar*H*), 8.08 (dd, $^3J$ = 8.5 Hz, $^4J$ = 1.5 Hz, 2H, Ar*H*), 7.83 (d, $^3J$ = 8.5 Hz, 2H, Ar*H*), 4.35 (t, $^3J$ = 6.8 Hz, 4H, C$H_2$O), 1.79−1.73 (m, 4H, C$H_2$CH$_2$O), 1.53−1.45 (m, 4H, C$H_2$CH$_2$CH$_2$O), 0.98 (t, $^3J$ = 7.6 Hz, 6H, C$H_3$); $^{13}$C NMR (125 MHz, DMSO-$d_6$) $\delta$ 166.5, 141.9, 126.2, 125.9, 123.4, 122.2, 120.8, 120.7, 112.8, 111.6, 64.0, 30.5, 18.9, 13.7; EIMS *m*/*z* 456.2055 [M]$^+$.

**11,12-Dihydroindolo[2,3-*a*]carbazole-3,8-dicarboxylic Acid (3).** Dibutyl 11,12-dihydroindolo[2,3-*a*]carbazole-3,8-dicarboxylate (**2**) (1.9 g, 4.2 mmol) was suspended in 2-propanol (40 mL), and a solution of KOH (23 g, 410 mmol) in $H_2O$ (80 mL) was added. The mixture was heated under reflux for 48 h, by which time the substrate had dissolved to give a clear, yellow biphasic solution. This was filtered, and 1 M $HCl_{(aq.)}$ was added to the filtrate until pH 7. The resulting precipitate was collected by filtration, washed with $H_2O$ (5 × 40 mL) followed by MeOH (2 × 15 mL), and dried under high vacuum to yield the product as a yellow powder (1.3 g, 91%): mp >300 °C; $^1$H NMR (500 MHz, DMSO-$d_6$) $\delta$ 12.61 (br s, 2H, COO*H*), 11.51 (s, 2H, N*H*), 8.83 (d, $^3J$ = 1.3 Hz, 2H, Ar*H*), 8.09 (s, 2H, Ar*H*), 8.03 (dd, $^3J$ = 8.5 Hz, $^4J$ = 1.6 Hz, 2H, Ar*H*), 7.78 (d, $^3J$ = 8.5 Hz, 2H, Ar*H*); $^{13}$C NMR (125 MHz, DMSO-$d_6$) $\delta$ 168.1, 141.7, 126.2, 126.1, 123.4, 122.2, 121.5, 120.8, 112.7, 111.4; EIMS *m*/*z* 344.0808 [M]$^+$.

(36) van Ameijde, J.; Liskamp, R. M. J. *Org. Biomol. Chem.* **2003**, *1*, 2661–2669.
(37) Hu, Y. Z.; Chen, Y. Q. *Synlett* **2005**, 42–48.

**Bis(2-(2-(2-hydroxyethoxy)ethoxy)ethyl) 11,12-Dihydroindolo-[2,3-*a*]carbazole-3,8-dicarboxylate (4).** 11,12-Dihydroindolo-[2,3-*a*]carbazole-3,8-dicarboxylic acid (**3**) (0.10 g, 0.29 mmol) was dissolved in dry, degassed DMF (4 mL), and the mixture was purged with $N_2$ for 20 min. Dry $Et_3N$ (1 mL, 7.2 mmol) and 2-[2-(2-chloroethoxy)ethoxy]ethanol (0.21 mL, 1.4 mmol) were added *via* syringe. The mixture was heated to 140 °C using microwave irradiation for 3 h. After cooling to room temperature, the solvent was removed *in vacuo* to leave a pale yellow oil. This was dry-loaded onto silica and purified by column chromatography ($SiO_2$; 5% MeOH in $CH_2Cl_2$). After drying under high vacuum, the product was obtained as a waxy white solid (0.12 g, 69%): mp 158−160 °C; $^1$H NMR (500 MHz, DMSO-$d_6$) $\delta$ 11.63 (s, 2H, N*H*), 8.85 (d, $^4J$ = 1.5 Hz, 2H, Ar*H*), 8.12 (s, 2H, Ar*H*), 8.05 (dd, $^3J$ = 8.4 Hz, $^4J$ = 1.5 Hz, 2H, Ar*H*), 7.81 (d, $^3J$ = 8.4 Hz, 2H, Ar*H*), 4.59 (br t, 2H O*H*), 4.47−4.43 (m, 4H, $CO_2CH_2$), 3.83−3.80 (m, 4H, C$H_2$), 3.67−3.64 (m, 4H, C$H_2$), 3.59−3.56 (m, 4H, C$H_2$), 3.51−3.40 (m, 8H, C$H_2$); $^{13}$C NMR (125 MHz, DMSO-$d_6$) $\delta$ 166.5, 142.0, 126.3, 126.0, 123.4, 121.1, 120.81 120.5, 112.8, 111.7, 72.4, 70.0, 69.8, 68.6, 63.7, 60.2; ESMS *m*/*z* 631.2262 $[M + Na]^+$.

**3,8-Dimethoxyindolocarbazole (5).** 1,2-Cyclohexanedione (0.56 g, 5.0 mmol) and 4-methoxyphenylhydrazine hydrochloride (2.6 g, 15 mmol) were dissolved in EtOH (50 mL), and concentrated $H_2SO_4$(aq) (1 mL) was added dropwise *via* syringe. The solution was heated to reflux for 18 h, and then $H_2O$ (200 mL) was added. After stirring at room temperature for 60 min, the precipitate was filtered and washed with $H_2O$ (5 × 15 mL). It was then dry-loaded onto silica and purified by column chromatography ($SiO_2$; hexane: ethyl acetate 9:1 graded to 7:3). The solvent was evaporated *in vacuo* to yield the product as a white solid (0.28 g, 18%): mp >250 °C; $^1$H NMR (500 MHz, DMSO-$d_6$) $\delta$ 10.88 (s, 2H, N*H*), 7.88 (s, 2H, Ar*H*), 7.72 (d, $^4J$ = 2.5 Hz, 2H, Ar*H*), 7.60 (d, $^3J$ = 8.5 Hz, 2H, Ar*H*), 7.03 (dd, $^3J$ = 8.5 Hz, $^4J$ = 2.5 Hz, 2H, Ar*H*), 3.88 (s, 6H, C$H_3$); $^{13}$C NMR (125 MHz, DMSO-$d_6$) $\delta$ 153.3, 133.8, 126.5, 124.3, 120.0, 113.7, 112.2, 111.3, 102.3, 55.6; EIMS *m*/*z* 316.1215 $[M^+]$.

**11,12-Dihydroindolo[2,3-*a*]carbazole-3,8-diol (6).** 3,8-Dimethoxy-11,12-dihydroindolo-[2,3-*a*]carbazole (**5**) (0.080 g, 0.25 mmol) was suspended in dry $CH_2Cl_2$ (10 mL) and the mixture was cooled to −78 °C. $BBr_3$ (1.0 mL of a 1 M solution in $CH_2Cl_2$, 1.0 mmol) was added. The reaction mixture was stirred at −78 °C for 30 min and then allowed to warm to room temperature and stirred for 16 h. Methanol (5 mL) was added, and the mixture was stirred for a further 60 min. The solvent was then removed *in vacuo*, and the residual solid was suspended in $CH_2Cl_2$: MeOH 9:1 (10 mL). After removal of the solvent *in vacuo*, the residual solid was suspended in $CH_2Cl_2$:MeOH 9:1 (10 mL). The suspension was filtered, and the solid was washed with $CH_2Cl_2$ (3 × 5 mL) and dried under high vacuum to give the product as a white solid (0.056 g, 77%): mp >250 °C; $^1$H NMR (500 MHz, DMSO-$d_6$) $\delta$ 10.67 (s, 2H, N*H*), 8.96 (s, 2H, O*H*), 7.71 (s, 2H, Ar*H*), 7.48 (d, $^3J$ = 8.5 Hz, 2H, Ar*H*), 7.44 (d, $^4J$ = 2.4 Hz, 2H, Ar*H*), 6.89 (dd, $^3J$ = 8.5 Hz, $^4J$ = 2.4 Hz, 2H, Ar*H*); $^{13}$C NMR (75 MHz, DMSO-$d_6$) $\delta$ 150.7, 133.1, 126.5, 124.6, 119.7, 113.9, 111.9, 111.0, 104.3; EIMS *m*/*z* 288.0886 $[M^+]$.

**2,2′-(2,2′-(2,2′-(11,12-Dihydroindolo[2,3-*a*]carbazole-3,8-diyl)-bis(oxy)bis(ethane-2,1-diyl))bis(oxy)bis(ethane-2,1-diyl))bis(oxy)diethanol (8).** Dry, degassed DMF was added to 11,12-dihydroindolo[2,3-*a*]carbazole-3,8-diol (**6**) (0.13 g, 0.45 mmol), 2-(2-(2-hydroxyethoxy)ethoxy)ethyl 4-methylbenzenesulfonate (**7**) (2.8 g, 9.2 mmol), and $K_2CO_3$, and the mixture was heated to 70 °C under a $N_2$ atmosphere for 60 h. The reaction mixture was poured onto $H_2O$ (40 mL), and the resultant precipitate was collected by filtration, washed with $H_2O$ (3 × 20 mL), and dried under suction on the frit for 60 min. The solid was then dissolved in THF, dry-loaded onto silica, and purified by column chromatography ($SiO_2$; EtOAc graded to EtOAc:MeOH 9:1). The pure fractions were concentrated *in vacuo*, and the residue was dried under high vacuum to yield the product as a waxy white solid (0.040 g, 16%): $^1$H NMR (500 MHz, DMSO-$d_6$) $\delta$ 10.90 (s, 2H, N*H*), 7.87 (s, 2H, Ar*H*), 7.74 (d, $^4J$ = 2.2 Hz, 2H, Ar*H*), 7.59 (d, $^3J$ = 8.8 Hz, 2H, Ar*H*), 7.04 (dd, $^3J$ = 8.8 Hz, $^4J$ = 2.2 Hz, 2H, Ar*H*), 4.65 (t, $^3J$ = 5.4 Hz, 2H, O*H*), 4.22−4.20 (m, 4H, C$H_2$), 3.83−3.81 (m, 4H, C$H_2$), 3.65−3.64 (m, 4H, C$H_2$), 3.59−3.57 (m, 4H, C$H_2$), 3.52−3.48 (m, 4H, C$H_2$), 3.46−3.44 (m, 4H, C$H_2$); $^{13}$C NMR (75 MHz, DMSO-$d_6$) $\delta$ 152.4, 133.9, 126.5, 124.3, 120.0, 114.2, 112.2, 111.4, 103.4, 72.4, 70.0, 69.9, 69.3, 67.8, 60.3; ESMS *m*/*z* 575.2365 $[M + Na]^+$.

***N*$^1$,*N*$^3$-Bis(3-bromopropyl)isophthalamide 9.** 3-Bromopropylamine hydrobromide (8.0 g, 37 mmol) was suspended in $CH_2Cl_2$ (120 mL), and $Et_3N$ (12 mL) was added. The solution was cooled to 0 °C, and isophthaloyl dichloride (3.7 g, 18 mmol) was added as a solid in one portion. The reaction mixture was stirred at 0 °C for 20 min. It was then allowed to warm to room temperature and stirred for 60 min. The reaction mixture was washed with 10% HCl(aq) solution (3 × 100 mL), saturated $NaHCO_3$(aq) (2 × 100 mL), $H_2O$ (2 × 100 mL), and brine (1 × 100 mL), dried over $MgSO_4$, and concentrated in vacuo to give the product as a white solid (2.6 g, 35%): mp 102−104 °C; $^1$H NMR (500 MHz, $CDCl_3$) $\delta$ 8.19 (t, $^4J$ = 1.8 Hz, 1H, ArH), 7.93 (dd, $^3J$ = 7.8 Hz, $^4J$ = 1.8 Hz, 2H, ArH), 7.54 (t, $^3J$ = 7.8 Hz, 1H, ArH), 6.52 (br t, 2H, NH), 3.64−3.60 (m, 4H, $CH_2$), 3.48 (t, $^3J$ = 6.4 Hz, 4H, $CH_2$), 2.22−2.17 (m, 4H, $CH_2$); $^{13}$C NMR (75 MHz, $CDCl_3$) $\delta$ 166.8, 134.6, 130.0, 129.1, 125.3, 38.8, 32.0, 30.9; FIMS *m*/*z* 406.01 $[M]^+$. Anal. Calcd for $C_{14}H_{18}N_2O_2Br_2$: C, 41.40; H, 4.47; N, 6.90. Found: C, 41.35; H, 4.45; N, 6.85.

**Compound 10.** A solution of 4,4′-bipyridine (8.7 g, 56 mmol) and *N*$^1$,*N*$^3$-bis(2-bromoethyl)isophthalamide (**9**) (5.6 g, 14 mmol) in $CH_3CN$ (250 mL) was heated to reflux for 24 h. After cooling to room temperature, the solvent was removed *in vacuo*, and the resulting yellow solid was purified by column chromatography ($SiO_2$; MeOH:$H_2O$:sat. $NH_4Cl$(aq) 6:3:1). After concentration of the pure fractions, the residual white solid was dissolved in $H_2O$, and saturated aqueous $NH_4PF_6$ was added until no further precipitation was observed. The precipitate was collected filtration, washed with $H_2O$ (4 × 20 mL) followed by MeOH (3 × 10 mL), and dried under high vacuum to yield the product as a white solid (8.7 g, 74%): mp 117 °C; $^1$H NMR (300 MHz, DMSO-$d_6$) $\delta$ 9.27 (d, $^3J$ = 7.0 Hz, 4H, Ar*H*), 8.86 (d, $^3J$ = 6.2 Hz, 4H, Ar*H*), 8.70 (t, $^3J$ = 5.3 Hz, 2H, N*H*), 8.63 (d, $^3J$ = 7.0 Hz, 4H, Ar*H*), 8.28 (br t, 1H, Ar*H*), 8.00 (d, $^3J$ = 6.2 Hz, 4H, Ar*H*), 7.94 (dd, $^3J$ = 7.9 Hz, $^4J$ = 1.8 Hz, 2H, Ar*H*), 7.54 (t, $^3J$ = 7.9 Hz, 1 H, Ar*H*), 4.71 (t, $^3J$ = 6.7 Hz, 4H, C$H_2$), 3.35−3.32 (m, 4H, C$H_2$), 2.28−2.24 (m, 4H, C$H_2$); $^{13}$C NMR (75 MHz, DMSO-$d_6$) $\delta$ 166.0, 152.4, 151.0, 145.5, 140.8, 134.4, 129.7, 128.3, 126.5, 125.3, 121.9, 58.7, 36.2, 30.7; $^{19}$F NMR (282 MHz, DMSO-$d_6$) $\delta$ 70 (d, $J$ = 712 Hz); $^{31}$P NMR (122 MHz, DMSO-$d_6$) $\delta$ −144 (septet, $J$ = 712 Hz); ESMS *m*/*z* 703.2367 $[M - PF_6]^+$.

**Macrocycle 1. Method 1.** A solution of compound **10** (0.30 mg, 0.35 mmol) in $CH_3CN$ (40 mL) and a solution of 1,4-bis(bromomethyl)benzene (0.092 g, 0.35 mmol) in $CH_3CN$ (40 mL) were simultaneously added to refluxing $CH_3CN$ (15 mL) over a 24 h period using a syringe pump. The reaction mixture was heated at reflux for a further 24 h before being concentrated *in vacuo*. The residual yellow solid was purified by column chromatography ($SiO_2$; $CH_3CN$:$H_2O$:sat. $KNO_3$(aq) 5:3:2). The pure fractions were evaporated to dryness, and the solid was dissolved in $H_2O$ (5 mL). A saturated aqueous solution of $NH_4PF_6$ was added until no further precipitate was observed. The precipitate was collected by filtration, washed with $H_2O$ (5 × 10 mL), and dried under high vacuum to yield the product as a white solid (0.16 g, 37%). The characterization data for this compound match those for the compound obtained *via* the method described below.

**Method 2.** Compound **10** (0.10 g, 0.12 mmol), 1,4-bis(bromomethyl)benzene (0.31 g, 0.12 mmol), and 2,2′-(2,2′-(1,4-phenylenebis(oxy))bis(ethane-2,1-diyl))bis(oxy)diethanol (0.34 g, 0.12 mmol) were dissolved in $CH_3CN$ (10 mL) under $N_2$. The reaction mixture was stirred at room temperature under $N_2$ for 7 days. The solvent was removed *in vacuo*, and the residual red solid was

purified according to the procedure described in method 1 above to afford the product as a white solid (0.063 g, 43%): mp >210 °C dec; $^1$H NMR (500 MHz, DMSO-$d_6$) $\delta$ 9.57 (d, $^3J$ = 7.3 Hz, 4H, Ar*H*), 9.39 (d, $^3J$ = 6.8 Hz, 4H, Ar*H*), 8.77 (d, $^3J$ = 7.3 Hz, 4H, Ar*H*), 8.73 (d, $^3J$ = 6.8 Hz, 4H, Ar*H*), 8.71 (t, $^3J$ = 5.4 Hz, 1H, N*H*), 8.11 (br t, 1H, Ar*H*), 7.96 (dd, $^3J$ = 7.8 Hz, $^4J$ = 2.0 Hz, 2H, Ar*H*), 7.82 (s, 4H, Ar*H*), 7.59 (t, $^3J$ = 7.8 Hz, 1H, Ar*H*), 5.95 (s, 4H, C$H_2$), 4.75 (t, $^3J$ = 6.4 Hz, 4H, C$H_2$), 3.20−3.16 (m, 4H, C$H_2$), 2.25−2.20 (m, 4H, C$H_2$); $^{13}$C NMR (75 MHz, DMSO-$d_6$) $\delta$ 166.0, 149.0, 148.5, 145.9, 145.5, 135.7, 134.4, 130.1, 129.3, 128.4, 127.2, 127.2, 126.5, 63.2, 58.4, 35.2, 30.3; $^{19}$F NMR (282 MHz, DMSO-$d_6$) $\delta$ 70 (d, $J$ = 712 Hz); $^{31}$P NMR (122 MHz, DMSO-$d_6$) $\delta$ −144 (septet, $J$ = 712 Hz); ESMS *m*/*z* 1097.2291 [M − $PF_6$]$^+$.

**Isocyanate Stopper 14.** 4-(Bis(4-*tert*-butylphenyl)(phenyl)-methyl)aniline (**13**) (0.12 g, 0.27 mmol) and triphosgene (0.040 g, 0.13 mmol) were dissolved in dry toluene (40 mL), and distilled triethylamine (0.040 mL, 0.29 mmol) was added. The solution was heated to 70 °C under a $N_2$ atmosphere for 4 h, filtered to remove triethylamine hydrochloride, and concentrated *in vacuo* to give the product as a pale yellow oil, which was dried under high vacuum for 60 min before being used immediately in the next step without further purification or characterization.

**Stoppered Axle 16.** Bis(2-(2-(2-hydroxyethoxy)ethoxy)ethyl) 11,12-dihydroindolo[2,3-*a*]carbazole-3,8-dicarboxylate **4** (0.035 g, 0.058 mmol) was dissolved in dry $CH_3CN$ (15 mL) under $N_2$ with the aid of vigorous heating and sonication. After cooling to room temperature, a solution of isocyanate stopper **14** (0.065 g, 0.14 mmol) in dry $CH_3CN$ (5 mL) was added *via* syringe. Di-*n*-butyltin dilaurate (2 drops) was then added, and the solution was stirred at room temperature under $N_2$ for 48 h. The solvent was removed *in vacuo*, and the residual solid was purified by column chromatography ($SiO_2$; 2% MeOH in $CH_2Cl_2$). After recrystallization from hot $CH_3CN$, the product was obtained as a white solid (0.077 g, 86%): mp >250 °C dec; $^1$H NMR (500 MHz, DMSO-$d_6$) $\delta$ 11.70 (s, 2H, indol-N*H*), 9.77 (s, 2H, OCON*H*), 8.87 (d, $^4J$ = 1.5 Hz, 2H, Ar*H*), 8.09 (s, 2H, Ar*H*), 8.07 (dd, $^3J$ = 8.8 Hz, $^4J$ = 1.5 Hz), 7.81 (d, $^3J$ = 8.5 Hz, 2H, Ar*H*), 7.35 (d, $^3J$ = 8.8 Hz, 4H, Ar*H*), 7.29−7.26 (m, 12H, Ar*H*), 7.18−7.14 (m, 6H, Ar*H*), 7.07−7.02 (m, 12H, Ar*H*), 4.44−4.42 (m, 4H, C$H_2$), 4.19−4.18 (m, 4H, C$H_2$), 3.82−3.80 (m, 4H, C$H_2$), 3.67−3.65 (m, 8H, C$H_2$), 3.62−3.60 (m, 4H, C$H_2$), 1,21 (s, 36H, C$H_3$); $^{13}$C NMR (125 MHz, DMSO-$d_6$) $\delta$ 166.5, 153.5, 147.8, 146.9, 143.7, 141.9, 140.7, 136.7, 130.7, 130.3, 130.0, 127.6, 126.3, 126.0, 125.7, 124.4, 123.4, 122.1, 120.8, 120.4, 117.6, 112.7, 111.6, 69.9, 69.8, 68.8, 68.6, 63.7, 63.5, 63.1, 34.0, 31.3; MALDI-TOF MS *m*/*z* 1555 98 [M]$^+$; ESMS *m*/*z* 1578.70 [M + Na]$^+$.

**[2]Rotaxane 15. Method 1.** Bis(2-(2-(2-hydroxyethoxy)ethoxy)-ethyl) 11,12-dihydroindolo[2,3-*a*]carbazole-3,8-dicarboxylate (**4**) (0.50 g, 0.082 mmol) was suspended in dry $CH_3CN$ (20 mL) under an atmosphere of $N_2$, and the suspension was heated and sonicated until it had formed a homogeneous solution. After cooling to room temperature, macrocycle **1** (0.10 g, 0.082 mmol) was added as a solid, followed by di-*n*-butyltin dilaurate (3 drops). A solution of isocyanate stopper **14** (0.16 g, 0.34 mmol) in dry $CH_3CN$ (10 mL) was then added, and the flask was wrapped with foil to protect the reaction mixture from light. After stirring at room temperature under $N_2$ for 60 h, the solvent was removed under reduced pressure without applying heat. The residue was dissolved in acetone and purified on a plug of silica, using acetone to elute high-running impurities before elution of the product using a saturated solution of $NH_4PF_6$ in acetone. The purple fractions were combined and concentrated to a volume of 2 mL, and then $H_2O$ (20 mL) was added. The purple precipitate was collected by filtration and washed with $H_2O$ (4 × 15 mL). It was then purified by column chromatography ($SiO_2$; saturated solution of $NH_4PF_6$ in acetone). The pure fractions were combined and concentrated to a volume of 2 mL, and then $H_2O$ (20 mL) was added to precipitate the product. This was collected by filtration, washed with $H_2O$ (10 × 15 mL) followed by EtOH (2 × 10 mL), and dried under high vacuum to afford the product as a purple solid (0.43 g, 19%). The characterization data for this compound match those for the compound obtained *via* the method described below.

**Method 2.** Stoppered axle **16** (0.060 g, 0.039 mmol) was dissolved in dry $CH_3CN$ (5 mL) under $N_2$, and 1,4-bis(bromomethyl)benzene (0.010 g, 0.038 mmol) and compound **10** (0.033 g, 0.039 mmol) were added. The reaction mixture was stirred at room temperature under $N_2$ for 10 days, during which time it slowly developed a purple color. The solvent was removed by evaporation without applying heat, and the residual solid was purified by column chromatography ($SiO_2$; saturated solution of $NH_4PF_6$ in acetone). The pure fractions were combined and concentrated to a volume of 2 mL, and $H_2O$ (20 mL) was added to precipitate the product, which was collected by filtration, washed with $H_2O$ followed by EtOH, and dried under high vacuum (0.0112 g, 10%): mp >140 °C dec; UV/vis ($CH_3CN$) $\lambda_{max}$ ($\epsilon$) = 260 (55 040 mol$^{-1}$ dm$^3$ cm$^{-1}$), 498 nm (890 mol$^{-1}$ dm$^3$ cm$^{-1}$); $^1$H NMR (500 MHz, $CD_3CN$) $\delta$ 10.72 (br s, 2H, N*H*), 8.95 (d, $^3J$ = 7.8 Hz, 4H, Ar*H*), 8.86 (br s, 2H, N*H*), 8.49 (d, $^3J$ = 7.3 Hz, 4H, Ar*H*), 8.24 (s, 4H, Ar*H*), 8.13 (d, $^3J$ = 7.6 Hz, 2H, Ar*H*), 8.07 (s, 2H, Ar*H*), 7.98 (d, $^3J$ = 8.8 Hz, 2H, Ar*H*), 7.88 (br t, 1H, Ar*H*), 7.80 (t, $^3J$ = 7.6 Hz, 1H, Ar*H*), 7.63 (s, 2H, N*H*), 7.40−7.38 (m, 6H, Ar*H*), 7.30 (d, $^3J$ = 8.3 Hz, 8H, Ar*H*), 7.23−7.19 (m, 12H, Ar*H*), 7.15−7.12 (m, 14H, Ar*H*), 7.07 (d, $^3J$ = 7.3 Hz, 4H, Ar*H*), 5.89 (s, 4H, C$H_2$), 5.59 (br s, 2H, Ar*H*), 4.66−4.64 (m, 4H, C$H_2$), 4.48 (br t, 4H, C$H_2$), 4.13−4.11 (m, 4H, C$H_2$), 4.06−4.04 (m, 4H, C$H_2$), 3.86−3.84 (m, 4H, C$H_2$), 3.77−3.75 (m, 4H, C$H_2$), 3.70−3.68 (m, 4H, C$H_2$), 3.50−3.48 (m, 4H, C$H_2$), 2.36−2.34 (m, 4H, C$H_2$), 1.23 (s, 36H, C$H_3$); $^{13}$C NMR (125 MHz, $CD_3CN$) $\delta$ 166.7, 153.6, 148.6, 147.6, 147.5, 145.1, 144.9, 144.2, 142.1, 136.2, 131.5, 131.1, 130.5, 130.2, 129.3, 127.6, 126.7, 126.4, 125.8, 125.1, 124.6, 122.6, 121.8, 121.5, 111.7, 111.4, 70.5, 70.4, 69.3, 69.0, 64.7, 64.3, 64.1, 63.6, 58.6, 47.1, 35.4, 34.0, 31.7, 30.5, 29.4, 29.3, 29.1, 29.0; $^{19}$F NMR (282 MHz, $CD_3CN$) $\delta$ 73 (d, $J$ = 712 Hz); $^{31}$P NMR (202 MHz, $CD_3CN$) $\delta$ −143 (septet, $J$ = 712 Hz); ESMS *m*/*z* 2652.79 [M − $PF_6$]$^+$, 2506.84 [M − 2$PF_6$]$^+$, 2361.89 [M − 3$PF_6$]$^+$.

**Crystal Structure Data. Macrocycle 1.** Moiety formula $C_{46}H_{48}N_8O_2$, 4($PF_6$), 2($C_2H_3N$), 7($CH_3CN$), $M$ = 1324.79, $Z$ = 4, monoclinic, space group $P2_1/c$, $a$ = 23.8889(2) Å, $b$ = 8.28350(10) Å, $c$ = 29.5789(3) Å, $\beta$ = 107.8184(4)°, $V$ = 5572.41(10) Å$^3$, $T$ = 150(2) K, $\mu$ = 0.262 mm$^{-1}$. Of 57 624 reflections measured, 12 568 were independent ($R_{int}$ = 0.070); final $R$ = 0.0737 (6695 reflections with $I > 2\sigma(I)$) and w$R$ = 0.0739. Data were collected on an Enraf-Nonius Kappa-CCD diffractometer under an open flow of $N_2$ gas at 150 K[38] and processed using the DENZO/SCALEPACK software.[39] The needle-like morphology of the crystals meant cutting caused damage, the crystal was too large for the homogeneous part of the X-ray beam, and the volume illuminated will have varied during the data collection. However, these were taken into account[40] by the multiscan interframe scaling.[39] The structures were solved by direct methods using the program SIR92,[41] and full-matrix least-squares refinement on $F$ was carried out using the CRYSTALS suite.[42] In general, all non-hydrogen atoms were refined with anisotropic displacement parameters except where there was disorder such that it was necessary to model the minor component as isotropic. Vibrational restraints, similar displacement restraints, and same distance restraints were used to maintain sensible geometries and atomic displacement ellipses for the other disordered components. Hydrogen atoms were visible in the difference map

(38) Cosier, J.; Glazer, A. M. *J. Appl. Crystallogr.* **1986**, *19*, 105–107.
(39) Otwinowski, Z.; Minor, W. In *Methods in Enzymology*; Carter, C. W., Sweet, R. M., Eds.; Academic Press: New York, 1997; Vol. 276, pp 307−326.
(40) Gorbitz, C. H. *Acta Crystallogr., Sect. B: Struct. Sci.* **1999**, *55*, 1090–1098.
(41) Altomare, A.; Cascarano, G.; Giacovazzo, C.; Guagliardi, A. *J. Appl. Crystallogr.* **1993**, *26*, 343–350.
(42) Watkin, D. J.; Prout, J. R.; Carruthers; Betteridge, P. W. *CRYSTALS*; Oxford, UK, 1996; Betteridge, P. W.; Carruthers, J. R.; Cooper, R. I.; Prout, K.; Watkin, D. J. *J. Appl. Crystallogr.* **2003**, *36*, 1487.

and were initially refined using soft restraints and then included in the refinement using a riding model.

**Pseudorotaxane.** Moiety formula $2(C_{42}H_{42}N_6O_2)$, $3(C_{18}H_{10}N_2)$, $8(PF_6)$, $7(CH_3CN)$, $M = 3535.60$, $Z = 4$, monoclinic, space group $P21/n$, $a = 20.1802(5)$ Å, $b = 28.0519(8)$ Å, $c = 29.3278(8)$ Å, $\beta = 108.36(1)°$, $U = 15757.2(7)$ Å$^3$, $T = 150(2)$ K, $\mu = 0.208$ mm$^{-1}$. Of 32 194 reflections measured, 32 146 were independent ($R_{int} = 0.039$); final $R = 0.1422$ (12 660 reflections with $I > 3\sigma(I)$) and w$R = 0.1570$). Crystals were small and weakly diffracting, so a synchrotron radiation source was used to collect diffraction data for this compound (at 150 K). Data were collected at Station 9.8, Daresbury SRS, UK, using a Bruker SMART CCD diffractometer. The structure was solved by direct methods using the program SIR92.[41]

The refinement and graphical calculations were performed using the CRYSTALS[42] and CAMERON[43] software packages. The structure was refined by full-matrix least-squares procedure on $F$. All non-hydrogen atoms were refined with anisotropic displacement parameters. Hydrogen atoms were located in Fourier maps and their positions adjusted geometrically (after each cycle of refinement) with isotropic thermal parameters. Chebychev weighting schemes and empirical absorption corrections were applied.[44] Treatment of 1.25 molecules of $H_2O$ (disordered) per asymmetric unit was performed using the procedure described by Spek[45] implemented in PLATON.[46] The structure contains solvent-accessible voids of 188.40 A$^3$ per unit cell, equivalent to ca. 1.25 molecules of $H_2O$ per asymmetric unit. Identification of the crystallizing solvent as water is based upon additional chemical evidence from $^1$H NMR. In view of the severe shortage of data, temperature factors have been refined isotropically for all $CH_3CN$ molecules and $PF_6^-$ counterions. There is disorder in all structure components including the encapsulated molecule, and a number of tight restraints needed to be applied (446 over 1761 parameters).

Crystallographic data for the structures reported in this paper have been deposited with the Cambridge Crystallographic Data Centre as supplementary publication no. CCDC 722648 and CCDC 722649. Copies of these data can be obtained free of charge from the Cambridge Crystallographic Data Centre *via* www.ccdc.cam.ac.uk/data_request/cif.

**Molecular Modeling.** Conventional molecular dynamic (MD) simulations were carried out with the AMBER10 software package.[47] Parameters for **15** and nitrate were taken from GAFF,[48] whereas DMSO was described using parameters reported by Kollman and Fox.[49] Van der Waals parameters for chloride,[50] bromide,[51] and iodide[51] were taken from the literature. Partial RESP[52]-fitted charges for nitrate and **15** were obtained from HF/6-31++G* and HF/6-31G* level geometry optimizations followed by single-point calculations at the same level of theory.[53] The starting model for the 1:1 association between chloride and **15** was obtained through assembly of the adequate individual moieties and then submitted to gas-phase quenched MD, consisting of a conventional 2 ns long MD at 2000 K, using a 1 fs time step, followed by molecular mechanics minimization of the resulting 20 000 structures. Minimization was performed through 1000 steps of the steepest descent method, followed by conjugate gradient until a convergence criterion of 0.0001 kcal mol$^{-1}$ was achieved. No bond or angle parameters were applied between the anions and the N−H binding sites, for which the attractive interactions were primarily electrostatic. The lowest energy structure with the thread unfolded thus obtained was further used in the condensed-phase MD simulations and as a template for the construction of the remaining supramolecular associations (therefore obtained by substitution of chloride by the adequate anion). These were then immersed in separate cubic boxes (typically ca. 60 Å in size after equilibration) containing approximately 1730 DMSO molecules. Charge neutralization was achieved by insertion of three hexafluorophosphate anions. MD simulations of the several systems started with an initial solvent and solute relaxation, followed by 50 ps NVT heating to 300 K and 500 ps NPT equilibration periods. The final densities of the equilibrated boxes were in close agreement with the experimental density of the solvent and remained constant during at least the final 300 ps of the NPT equilibration period. SHAKE was employed in all condensed-phase simulations to constrain all hydrogen-involving bonds, thus allowing the usage of 2 fs time steps. Nonbonded van der Waals interactions were restrained to a 12 Å cutoff, while the particle mesh Ewald method was used to describe the long-range electrostatic interactions. The temperature of the systems was controlled by the Langevin thermostat, using a collision frequency of 1.0 ps$^{-1}$.

The relative association free energies ($\Delta\Delta G$) of the [2]rotaxane **15** to chloride, bromide, and iodide were calculated from the relative free energies obtained for the solvated free anions (solvation free energy $-\Delta G_{solvation}$) and for the solvated rotaxane-bounded anions (interaction free energy $-\Delta G_{interaction}$) by means of thermodynamic integration[54,55] as

$$\Delta\Delta G = \Delta G_{solvation} - \Delta G_{interaction} \quad (1)$$

Similarly, the relative association entropies ($\Delta\Delta S$) were obtained from[54,56]

$$\Delta\Delta S = \Delta S_{solvation} - \Delta S_{interaction} \quad (2)$$

Perturbation calculations were divided into 21 windows ($\lambda = 0$, 0.05, 0.10, ..., 1). Each window consisted of a molecular dynamics simulation, divided into a 200 ps equilibration step followed by a data collection step of 200 ps for the free anions in DMSO and 300 ps for the anions in complexes, both carried out at 300 K and 1 atm using the previously equilibrated systems.

**Acknowledgment.** We thank Dr. N. H. Rees for NMR advice and the EPSRC for postdoctoral fellowships (K.M.M., M.J.C.) and a studentship (A.B.). S.M.S. acknowledges FCT for a Ph.D. grant (SFRH/BD/29596/2006). V.F. acknowledges the Fundação para a Ciência e Tecnologia (FCT), with coparticipation of the European Community funds FEDER, for the financial support under project PTDC/QUI/68582/2006. S.I.P. thanks the Royal Society for funding and SRS Daresbury for a research grant to support crystallographic work.

**Supporting Information Available:** $^1$H NMR spectra of all new compounds; $^{13}$C, $^{19}$F, and $^{31}$P NMR spectra and electrospray mass spectrum of [2]rotaxane **15**; aromatic stacking

(43) Watkin, D. J.; Prout, J. R.; Pearce, L. J. *CAMERON*; Oxford, UK, 1996.
(44) Walker, N.; Stuart, D. *Acta Crystallogr., Sect. A.* **1983**, *39*, 158–166.
(45) Spek, A. *J. Appl. Crystallogr.* **2003**, *36*, 7–13.
(46) Spek, A. L. *PLATON*, A Multipurpose Crystallographic Tool; Ultrecht, The Netherlands, 1998.
(47) Case, D. A.; et al. *AMBER 10*; University of California, San Francisco, 2008.
(48) Wang, J. M.; Wolf, R. M.; Caldwell, J. W.; Kollman, P. A.; Case, D. A. *J. Comput. Chem.* **2004**, *25*, 1157–1174.
(49) Fox, T.; Kollman, P. A. *J. Phys. Chem. B* **1998**, *102*, 8070–8079.
(50) Blas, J. R.; Marquez, M.; Sessler, J. L.; Luque, F. J.; Orozco, M. *J. Am. Chem. Soc.* **2002**, *124*, 12796–12805.
(51) Jorgensen, W. L.; Ulmschneider, J. P.; Tirado-Rives, J. *J. Phys. Chem. B* **2004**, *108*, 16264–16270.
(52) Bayly, C. I.; Cieplak, P.; Cornell, W. D.; Kollman, P. A. *J. Phys. Chem.* **1993**, *97*, 10269–10280.
(53) Frisch, M. J.; et al. *Gaussian 03*, Revision B.04; Gaussian Inc.: Walliingford, CT, 2004.
(54) Huang, B. Q.; Santos, S. M.; Felix, V.; Beer, P. D. *Chem. Commun.* **2008**, 4610–4612.
(55) Chipot, C.; Pohorille, A. *Free Energy Calculations—Theory and Applications in Chemistry and Biology*; Springer-Verlag: Berlin, 2007.
(56) Peter, C.; Oostenbrink, C.; van Dorp, A.; van Gunsteren, W. F. *J. Chem. Phys.* **2004**, *120*, 2652–2661.

distances from pseudorotaxane crystal structure; UV−vis and $^1$H NMR titration protocols and binding curves; probability distribution functions for the computed isophthalamide N−H···X, indolocarbazole N−H···X, and indolocarbazole···isophthalamide distances; absolute and relative solvation free energies of anions in DMSO from thermodynamic integration calculations; CIF files for the X-ray crystals structures; complete refs 22, 47, and 53. This material is available free of charge via the Internet at http://pubs.acs.org.

JA809905X